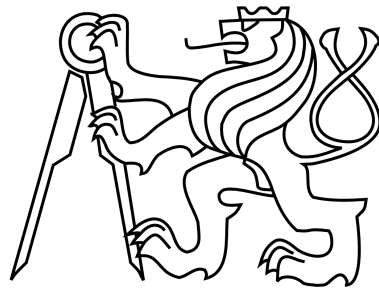


CZECH TECHNICAL UNIVERSITY IN PRAGUE

Faculty of Electrical Engineering



**MASTER'S THESIS**

CZECH TECHNICAL UNIVERSITY IN PRAGUE

Faculty of Electrical Engineering

Department of Telecommunication Engineering

# Path Selection for Delivery of Data from a User to Femto-cloud

Ing. Programme: Communication, Multimedia and Electronics  
Specialisation: Electronic Communication Networks

May 2014

Author: Bc. Jan Plachý  
Supervisor: doc. Ing. Zdeněk Bečvář, Ph.D.

České vysoké učení technické v Praze  
Fakulta elektrotechnická

katedra telekomunikační techniky

## ZADÁNÍ DIPLOMOVÉ PRÁCE

Student: **Bc. Plachý Jan**

Studijní program:  
Obor: Sítě elektronických komunikací

Název tématu: **Výběr cesty pro doručení dat od uživatele k femto-cloudu**

Pokyny pro vypracování:

Seznamte se s konceptem tzv. femto-cloudu a definujte parametry vhodné pro výběr nejvhodnější cesty pro doručení dat od uživatele k femtobuňkám tvořícím femto-cloud. Poté navrhnete způsob výběru přístupové stanice pro uživatele s ohledem na požadovaný typ služby a kvalitu komunikačních kanálů. Efektivitu navrženého algoritmu zhodnoťte pomocí simulací v prostředí MATLAB.

Seznam odborné literatury:

- [1] K.C. Chu, T.C. Huang, and L.C. Tsai,: A Path Selection Scheme Designed for Best-Effort Data Delivery in IEEE 802.16j Networks, International Conference on Wireless Communications, Networking and Mobile Computing (WiCOM), September 2011.
- [2] L. Liu, X. Li, J. Jin, Z. Huang, M. Liu, M. Palaniswami, Graph-Based Routing, Broadcasting and Organizing Algorithms for Ad-Hoc Networks, Wireless Ad-Hoc Networks, edited by Hongbo Zhou. December 2012.

Vedoucí: Ing. Zdeněk Bečvář, Ph.D.

Platnost zadání: do konce zimního semestru 2014/2015



prof. Ing. Boris Šimák, CSc.  
vedoucí katedry



prof. Ing. Pavel Ripka, CSc.  
děkan

V Praze dne 20. 11. 2013

I hereby declare that this master's thesis is completely my own work and that I used only the cited sources in accordance with the Methodical instruction about observance of ethical principles of preparation of university final projects.


Prague, May 12, 2014



Signature

Prohlašuji, že jsem předloženou práci vypracoval samostatně a že jsem uvedl veškeré použité informační zdroje v souladu s Metodickým pokynem o dodržování etnických principů při přípravě vysokoškolských závěrečných prací.

V Praze dne 25. Května 2014



Podpis

## **Acknowledgments**

I am deeply grateful to my supervisor doc. Ing. Zdeněk Bečvář, Ph.D., for his encouragement and invaluable guidance throughout the thesis and for the opportunity to work on a large research project. Also I would like to thank Ing. Pavel Mach, Ph.D. for his suggestions and other colleagues from the TROPIC project.

My thanks also belongs to my family for their love, support and understanding. Also I would like to thank especially to one person, who had the patience, pushed me through when I needed and made me believe everything is possible.

## Abstract

To overcome latency constrain of common mobile cloud computing, computing capabilities can be integrated into LTE enhanced NodeB (eNB) in mobile networks. This exploitation of convergence of mobile networks and cloud computing enables to take advantage of proximity between a user equipment (UE) and its serving station to lower latency and to avoid backhaul overloading due to cloud computing services. This concept of cloud-enabled small cells is known as small cell cloud (SCC). In this thesis, small cell cloud is investigated and algorithm for selection of path between the UE and the cell, which performs computing for this particular UE, is proposed. As a path selection metrics we consider transmission delay and energy consumed for offloaded data transmission. The path selection considering both metrics is formulated as a Markov Decision Process. Efficiency of proposed algorithm is simulated and compared to the existing algorithm.

**Key words :** Mobile cloud computing, Path selection, Energy efficiency, LTE

## Anotace

Pro snížení doby zpoždění v mobilním cloudu je možné do LTE základnových stanic přidat dodatečný výpočetní výkon pro potřeby cloudu. Tímto přidáním může uživatel využívat cloudové služby s menším zpožděním a taktéž nezatěžovat páteřní síť. Tento princip byl nazván jako cloud malých buněk. V rámci této diplomové práce, je prozkoumána problematika cloudu malých buněk a je navržen algoritmus pro výběr cesty k buňkám obsluhující požadavek uživatele. Jako váha pro výběr cesty je uvažováno zpoždění cesty a energetické nároky cesty. Navržený algoritmus vychází z Markovova rozhodovacího procesu. Efektivita algoritmu je simulací porovnána s existujícím algoritmem.

**Klíčová slova :** cloud malých buněk, výběr cesty, energetická efektivita, LTE

# Contents

<b>1</b>	<b>Introduction</b>	<b>1</b>
<b>2</b>	<b>Related works</b>	<b>2</b>
<b>3</b>	<b>System model</b>	<b>4</b>
3.1	Physical layer of LTE-A . . . . .	4
3.2	Small cells . . . . .	6
3.2.1	Handover procedure . . . . .	8
3.3	Small cell cloud . . . . .	9
3.3.1	SCC architecture . . . . .	9
3.3.2	Cloud request . . . . .	10
3.3.3	Small cell cloud manager . . . . .	11
<b>4</b>	<b>Proposed path selection algorithm for SCC</b>	<b>12</b>
4.1	Path selection algorithm . . . . .	12
4.2	Derivation of path selection parameters . . . . .	14
4.3	Management messages for exchange of the required information . . . . .	15
4.4	Algorithm complexity . . . . .	16
<b>5</b>	<b>System model and simulation methodology</b>	<b>17</b>
5.1	System model . . . . .	17
5.1.1	Transmission of offloaded data . . . . .	18
5.2	Simulation scenario and models . . . . .	19
5.2.1	Energy consumption model . . . . .	21
<b>6</b>	<b>Simulation results</b>	<b>26</b>
6.1	UE point of view . . . . .	26
6.2	Network point of view . . . . .	33
6.2.1	GBR . . . . .	33
6.2.2	Shared radio resources . . . . .	37
<b>7</b>	<b>Conclusion</b>	<b>42</b>
<b>8</b>	<b>Appendices</b>	<b>46</b>

# List of Figures

3.1	LTE-A TDD frame structure [1]. . . . .	4
3.2	LTE-A FDD frame structure [1]. . . . .	4
3.3	Time-frequency structure of FDD and TDD in LTE-Advanced [2]. . . . .	5
3.4	UE connection to the operator's network. . . . .	6
3.5	Small cell architecture. . . . .	7
3.6	HeNB and micro/picocell connection to the operator. . . . .	7
3.7	Basic handover procedure. . . . .	8
3.8	SCeNB handover variants. . . . .	9
3.9	Cluster architecture. . . . .	9
3.10	SCC request process. . . . .	10
4.1	Message to obtain available bandwidth and measure delay. . . . .	15
5.1	SCC system model. . . . .	18
5.2	Unused bits for handover duration 30 ms. . . . .	18
5.3	Simulation area. . . . .	20
5.4	Indoor movement. . . . .	20
5.5	UE to eNB communication. . . . .	22
5.6	Example of energy consumption ( $PL = 80dB$ , $10RBs$ , $100kB$ ) transmission. . . . .	24
5.7	Downlink power consumption. . . . .	25
6.1	Average delay $D$ required for transmission of offloaded computing task to computing cells for request size of 300kB. . . . .	26
6.2	Average delay $D$ required for transmission of offloaded computing task to computing cells for request size of 30 MB. . . . .	27
6.3	Average energy $E$ consumed by radio transmission of offloaded computing task to computing cells for request size of 300kB. . . . .	28
6.4	Average energy $E$ consumed by radio transmission of offloaded computing task to computing cells for request size of 30 MB. . . . .	28
6.5	Satisfaction of users with experienced delay for request size of 300 kB. . . . .	29
6.6	Satisfaction of users with experienced delay for request size of 30 MB. . . . .	30
6.7	Ratio of additional handovers due to proposed algorithm with respect to usage of serving cell only (SO). . . . .	31
6.8	Gain in delay against SO for optical fiber backhaul. . . . .	31
6.9	Gain in delay against SO for DSL backhaul. . . . .	32
6.10	Gain in energy against SO optical fiber backhaul. . . . .	32
6.11	Gain in energy against SO DSL backhaul. . . . .	33
6.12	Gain in delay against SO for request size of 300 kB. . . . .	34



---

6.13	Gain in delay against SO for request size of 3 MB. . . . .	34
6.14	Gain in energy against SO for request size of 300 kB. . . . .	35
6.15	Gain in energy against SO for request size of 3 MB. . . . .	35
6.16	UE satisfaction for request size of 300 kB. . . . .	36
6.17	UE satisfaction for request size of 3 MB. . . . .	36
6.18	Number of additional handovers for request size of 300 kB. . . . .	37
6.19	Number of additional handovers for request size of 3 MB. . . . .	37
6.20	Gain in energy against SO for request size of 300 kB. . . . .	38
6.21	Gain in energy against SO for request size of 3 MB. . . . .	38
6.22	Gain in delay against SO for request size of 300 kB. . . . .	39
6.23	Gain in delay against SO for request size of 3 MB. . . . .	39
6.24	UE satisfaction for request size of 300 kB. . . . .	40
6.25	UE satisfaction for request size of 3 MB. . . . .	40
6.26	Number of additional handovers for request size of 300 kB. . . . .	41
6.27	Number of additional handovers for request size of 3 MB. . . . .	41

# List of Tables

5.1	Distribution of time stay in specific rooms for indoor movement . . . .	21
5.2	Simulation parameters . . . . .	21
5.3	Backhaul parameters . . . . .	22
8.1	E-UTRA frequency bands [3] . . . . .	47
8.2	Assigned SINR to CQI . . . . .	48

# List of Acronyms

**3GPP** Third Generation Partnership Project.

**AMC** Adaptive Modulation and Coding.

**ANR** Automatic Neighbor Relation.

**AOMDV-DPU** Ad-hoc On-demand Multipath Distance Vector with Dynamic Path Update.

**CQI** Channel Quality Index.

**DSL** Digital Subscriber Line.

**E-UTRA** Evolved Universal Terrestrial Radio Access.

**eNodeB** enhanced NodeB.

**EPC** Evolved Packet Core.

**EPS** Evolved Packet System.

**FDD** Frequency Division Duplex.

**GBR** Guaranteed Bit ratio.

**HeNB** Home eNodeB.

**HeNB-GW** HeNB Gateway.

**HSS** Home Subscriber Server.

**LAN** Local Area Network.

**LTE** Long Term Evolution.

**LTE-Advanced** Long Term Evolution-advanced.

**MCS** Modulation Coding Scheme.

**MDP** Markov Decision Process.

**MIMO** Multiple Input Multiple Output.

**MME** Mobility Management Entity.

**NCL** Neighbor Cell List.

**NRT** Neighbor Relation Table.

**OFDM** Orthogonal Frequency Division Multiplex.

**OSN** Operator Service Network.

**PGW** Packet Data Network Gateway.

**PSwH** Path Selection with Handover.

**PUSCH** Physical Uplink Shared Channel.

**QAM** Quadrature Amplitude modulation.

**QoS** Quality of Service.

**QPSK** Quadrature Phase Shift Keying.

**RB** Resource Block.

**RSSI** Received Strength Signal Indicator.

**S-GW** Serving Gateway.

**SC** Small Cell Cloud Manager.

**SC-FDMA** Single Carrier-Frequency Division Multiple Access.

**SCC** Small Cell Cloud.

**SCeNB** Small Cell.

**SeGW** Security Gateway.

**SINR** Signal to Interference and Noise Ratio.

**SISO** Single Input Single Output.

**SO** Serving Only.

**SON** Self Organizing Network.

**TDD** Time Division Duplex.

**UE** User Equipment.

**VM** Virtual Machine.

**VoIP** Voice over IP.

**WSN** Wireless Sensor Networks.

# Introduction

As demands of mobile users are being shifted from hardware to software [4], opportunity for offloading computation from user equipment (UE) into cloud is becoming interesting possibility to provide enough computing power for even computationally demanding applications while saving battery of the UEs. However, conventional cloud computing approaches lead to a significant delay in delivery of offloaded data from the UE to computing machine and back [5]. Therefore, delay sensitive applications cannot be widely used in this scenario. As a solution to overcome the problem of delay in mobile cloud computing, cloud resources should be deployed closer to the users. In Long Term Evolution - Advanced (LTE-A) mobile networks, the closest place for deployment of computing resources is an enhanced NodeB (eNB).

With increasing trend in dense deployment of Small Cells [6], these are seen as a mean to provide cloud computing services to users in proximity. This concept is known as Small Cell Cloud (SCC) [7]. In the SCC, the small cells (SCeNB) are empowered by additional computing and storage resources. To satisfy even high demands of the UEs on computation, the computing power distributed over nearby cloud-enhanced SCeNBs can be virtually merged together under one Virtual Machine (VM). The application is then offloaded from the UE to the SCeNBs if it is profitable from energy or delay point of view [8]. The VMs are deployed at SCeNBs with respect to their communication and computation capabilities. After selection of the SCeNBs, which take care of computation, data must be delivered to these cells [9].

Typically, the small cells are usually connected to backhaul, which is of a lower quality than common backhaul of macrocells. Hence, distribution of data for computation from the cell providing radio access (serving cell) to all computing cells through backhaul of limited capacity can lead to significant delay. To that end, it is efficient to deliver data to selected computing cells not only through the serving cell but also by means of neighboring cells provided that those are in the user's radio communication range.

Goal of this thesis is to explore Small Cell Cloud, define the suitable parameters for path selection of data delivery and to design suitable path selection algorithm for the SCC, based on these parameters. Efficiency of proposed algorithm is to be proved by the simulation in MATLAB.

The rest of this paper is organized as follows. In the next section, we define model of the investigated SCC system. In Section III, the proposed algorithm for path selection is described. Simulation environment and results are presented in Section IV. The last section summarizes major conclusions and outlines plans for future extension of this work.

# Related works

The problem of selection of the most appropriate path for data delivery to the computing cells can be seen as an analogical problem to routing in Wireless Sensor Networks (WSN). Thus, the WSN routing protocols may provide an inspiration how to treat the path selection in the SCC. Of course, mobile network topology does not enable such freedom as conventional WSN but it rather follows hierarchical network structure in the WSN where some nodes are selected as gateways (cluster heads), which relay data to a target destination [10].

In mobile network, the SCeNBs can be seen as gateway nodes. Each gateway has a fix number of options how to distribute offloaded computation data to computing cells through fixed infrastructure of the mobile network. This infrastructure is represented typically by a wired backhaul and core network of the operator. Therefore, the problem consists in selection of a proper gateway (serving cell) for individual parts of offloaded data. The selected gateway must minimize data transmission delay and energy consumed by the UEs for the transmission. Note that the same problem can be defined also for delivery of computation results back to the UE (e.g., if the original path is not efficient due to user's movement).

In the WSN, plenty of algorithms have been defined. Basic routing algorithms for the WSN do not consider energy consumption of data delivery or dynamic path update [10]. In the SCC, the energy is limiting only for radio communication between the UE and the SCeNBs. Also, dynamics of the system is inherent feature of mobile networks. Therefore, energy as well as dynamics must be taken into account. Dynamics of scenario for the WSN is addressed, for example, by the Ad-hoc On-demand Multipath Distance Vector with Dynamic Path Update (AOMDV-DPU) [11]. Additionally to hop count metric, this algorithm selects paths based on the Received Strength Signal Indicator (RSSI). However, this algorithm does not consider transmission energy, which is essential in our case. Similar weakness prevents implementation of Adaptive Multi-metric Ad-Hoc On-Demand Multipath Distance Vector Routing algorithm [12] to the SCC since it routes data based only on RSSI, latency and node occupancy. Moreover, backhaul from the serving cell to the mobile operator's core network is typically wired. In addition, if serving cell selection is based on RSSI, the same path to the core network would be selected all the time disregarding selection of the SCeNBs for computation. It means that WSN-like approaches cannot be simply applied to our problem.

Designed path selection algorithm should take into account UE's limited energy resources, radio and backhaul conditions, and UE requirements on maximal possible delay using selected path to guarantee Quality of Service (QoS). In existing approaches used for delivery of offloaded data from the UE to the computing SCeNBs in the SCC, the data is always delivered to the computing cells through the serving cell [7],[9]. It means the UE is attached still to the same cell during delivery of all data. Then, the serving cell distributes data through operator's core networks to the computing cells. This approach can be efficient if both radio channel between the UE and its serving cell and backhaul connection of the serving as well as all computing cells is of sufficient

---

throughput. Otherwise, limitation at any part of the communication chain leads to a degradation of the overall delay of computation offloading.

# System model

In this chapter, the model of the SCC is presented in order to enable description of the path selection algorithm. Prior to explanation of architecture and fundamental idea of the SCC, brief overview of LTE-A mobile networks and small cells is briefly introduced.

## 3.1 Physical layer of LTE-A

As the SCC is technology designed for the future generation of mobile networks, we consider LTE-A for radio communication. The LTE-A in its latest version is frozen as a 3GPP release 11 [1].

The physical layer of the LTE-A defines two types of frames [1]: Time Division Duplex (TDD) and Frequency Division Duplex (FDD). The structure of both frames are shown in Figures 3.1 and 3.2.

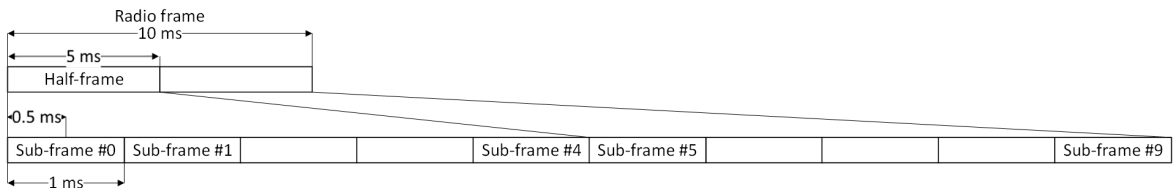


Figure 3.1: LTE-A TDD frame structure [1].

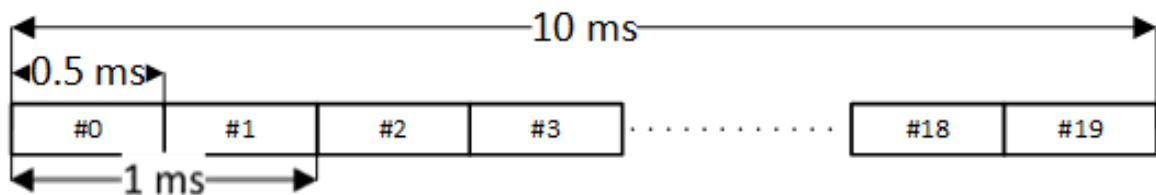


Figure 3.2: LTE-A FDD frame structure [1].

For the duplex communication in the TDD and the FDD (used frequency bands are shown in 8.1), switching between uplink and downlink or using two separate carrier frequencies, is shown in Figure 3.3. To switch between uplink and downlink in TDD, a special subframe consisting of a downlink part (DwPTS), a guard period (GP) and an uplink part (UpPTS) is defined in [1]. In case of used FDD, uplink and downlink occur on separate frequencies. Resource Block (RB) in the LTE-A is the smallest resource allocation unit assigned by the eNB scheduler.



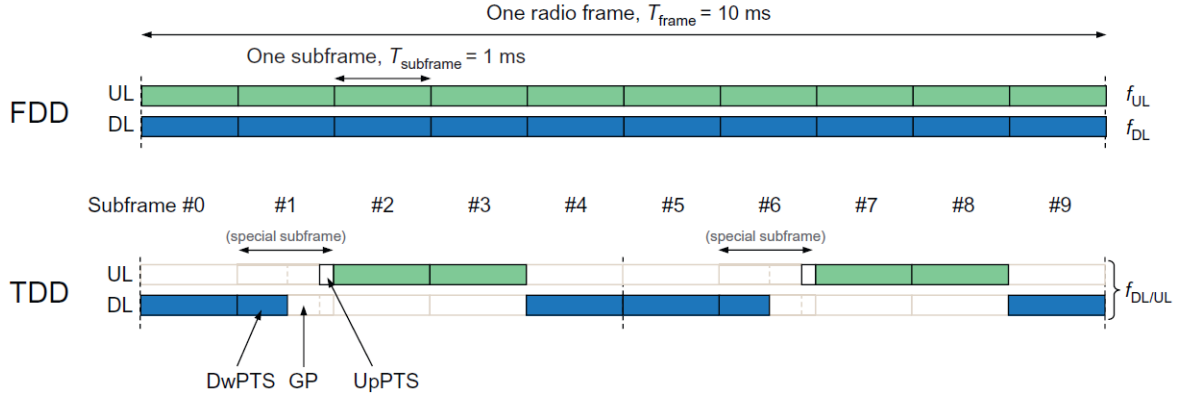


Figure 3.3: Time-frequency structure of FDD and TDD in LTE-Advanced [2].

For the LTE-A an Orthogonal Frequency Division Multiple Access (OFDMA) is used as a multi-carrier scheme that allocates radio resources to multiple users in the downlink. For the uplink, Single Carrier – Frequency Division Multiple Access (SC-FDMA) is utilized as it consumes less energy [13].

Several types of modulation, ranging from the Quadrature Phase Shift Keying (QPSK) to the 64-Quadrature Amplitude Modulation (QAM), and code rates as defined for transmission of more symbols per carrier in [1]. The selection of suitable Modulation and Coding Scheme (MCS) is based on mapping the MCS to the Signal to Interference plus Noise Ratio (SINR) and required Bit Error Rate (BER). This feature is known as the Adaptive Modulation and Coding (AMC). Maximal throughput of the LTE-A in 1x1 Multiple Input Multiple Output (MIMO) or Single Input Single Output (SISO) configuration is reached with 64-QAM and code rate of 948/1024 [14]. Maximal throughput using 20 MHz bandwidth with the 64-QAM modulation and the lowest redundancy for coding is roughly 100 Mbit/s for downlink direction, whereas for the uplink direction, only modulations up to 16-QAM can be used thus obtaining throughput of 50 Mbit/s.

The LTE-A Evolved Packet System (EPS) is shown in Figure 3.4 [15]. The EPS consists of the Evolved Universal Terrestrial Radio Access (E-UTRA) and the Evolved Packet Core (EPC). The E-UTRA is providing access network for the UE connected through the eNB. The EPC consists of the Serving Gateway (SGW), the Packet Data Network Gateway (PGW), the Mobility Management Entity (MME) and the Home Subscriber Server (HSS) [16]. There are two types of connections between components, the user plane, used for the user data and the control plane, used for the network signaling. The SGW is responsible for transport of the IP data traffic between the UE and the external networks (e.g. Internet). It also serves as the anchor point for the handovers between eNBs and between LTE-A and other 3GPP accesses. The PGW interconnects EPC with the external IP data networks and allocates IP addresses. The MME deals with the signaling related to mobility and security for E-UTRAN access. The HSS is a database filled with user-related and subscriber related information. It is also used for UE authentication and access authorization.

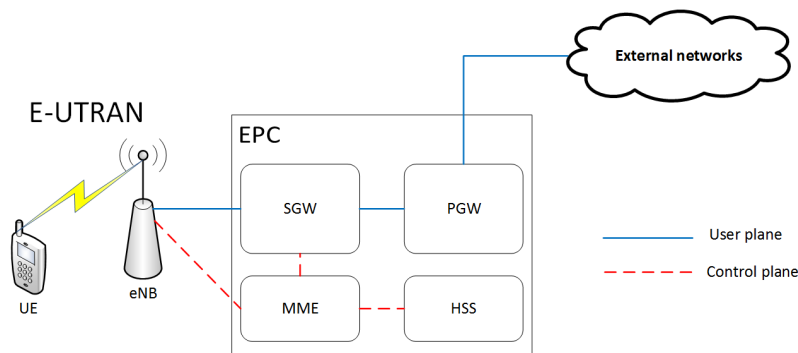


Figure 3.4: UE connection to the operator's network.

The Self Organizing Network (SON) introduced as a part of the 3GPP LTE-A is a key driver for involving operation & maintenance (O & M). The network should be optimized based on radio propagation, user traffic and mobility. To manage neighbor cell list (NCL) a scheme of Automatic Neighbor Relation (ANR) was standardized by the 3GPP [17]. ANR is used to detect and measure UE radio relations directly by UE. The neighbor relations are managed in a Neighbor Relation Table (NRT). As the user mobility is one of the most important issues in LTE-A, NCL is used for the purposes of handover (mobility) to select new serving eNB.

## 3.2 Small cells

With the increasing demand for mobile services [18], mobile network providers had to come up with new solutions to satisfy demands from users. Solutions to provide higher quality of mobile service are based on various techniques. One of the promising solution is densification of eNBs deployment. By deploying higher number of the eNBs, the operator increases area coverage and can offload users from highly utilized stations. However there are several drawbacks including the eNB cost and interference to other stations caused by the newly deployed eNB. Since eNBs are deployed by mobile operators they have to secure connection to their network and supply power for eNB.

To lower interference, while providing better coverage and services, smaller cells (e.g. microcells, picocells, or femtocells) can be deployed. To transfer cost of deployment, backhaul connection and consumed power the concept of femtocells (through this thesis femtocells are labeled HeNB) was introduced. HeNBs [19] are seen as the future of mobile networks from the operators point of view as they are deployed by the users, whom pay for its deployment as well provide backhaul connection and power supply. By doing so, users obtain some benefits from the operator (e.g. pay less for the services). Deployment by the users made several requirements on HeNBs as of self-deployment and self-configuration. With these requirements being addressed, HeNBs provide solution to dense deployment of eNBs while keeping low interference, transferring part of the cost to the customers and providing better service to the users. Example of SCeNBs deployment, including HeNBs as well as micro/pico cells, is shown in Figure 3.5 [20].

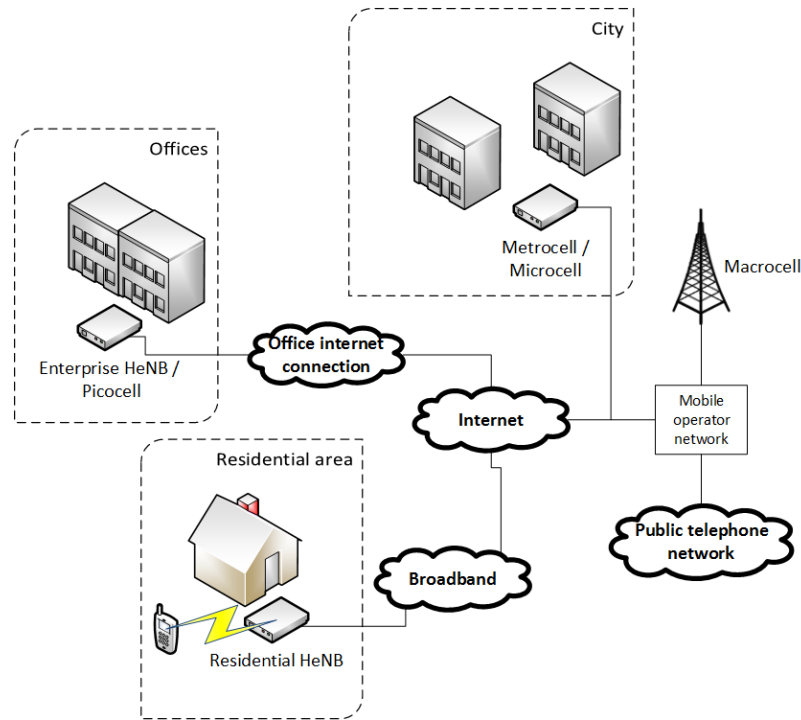


Figure 3.5: Small cell architecture.

SCeNBs are connected to the mobile operator using backhaul architecture as shown in Figure 3.6 from [21]. Microcells or picocells are connected directly to the SGW. The HeNBs are through the Internet connected to the HeNB Gateway (HeNB-GW), which allows an S1 interface between the HeNB and the EPC in order to support a large number of HeNBs in a scalable manner [2]. The S1 interface serves as a reference point, for the control plane protocol between the E-UTRAN and the MME, for user plane tunneling and handover purposes [16]. The Packet Data Network Gateway (PGW) is conjunction between 3GPP and non-3GPP technologies. From the PGW communication to the Operator Service Network (OSN) or the Internet is possible.

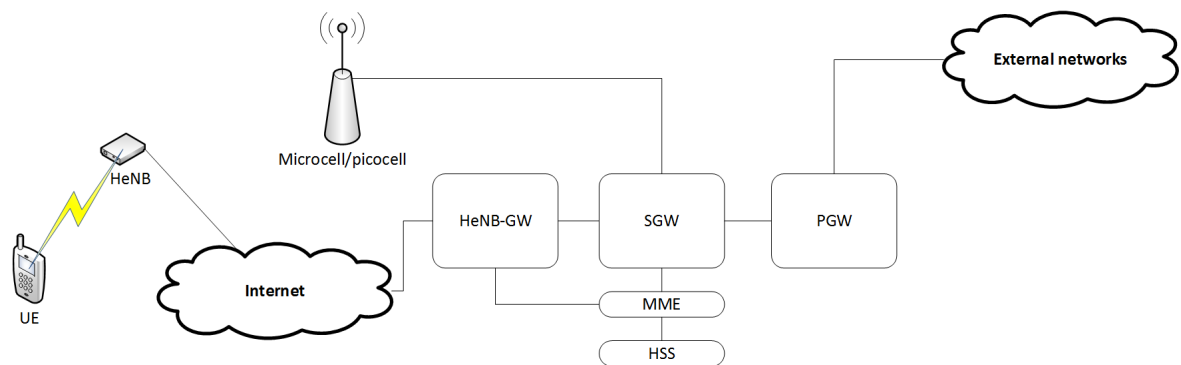


Figure 3.6: HeNB and micro/picocell connection to the operator.

As for the deployment of SCeNBs, two options are possible. SCeNBs can either have dedicated carrier frequencies or share carrier frequencies with other SCeNBs or eNBs. As the HeNBs use the same carrier frequencies as other cells in neighborhood, time, frequency and phase synchronization might be required as stated in [22]. As the LTE-A FDD system is used, frequency synchronization is required in order to

preserve orthogonality between the subcarriers. If LTE-A TDD is used, phase and time synchronizations are required to avoid interference between uplink and downlink transmissions. In [23] requirements on time synchronization are specified stating that synchronization error must be within  $3 \mu\text{s}$  or within  $10 \mu\text{s}$  if synchronization cell distance is above 500 m.

### 3.2.1 Handover procedure

To address user mobility, handover is used in mobile networks to provide seamless connection for the UE as it moves in space. To illustrate basic handover operation, brief introduction is provided.

When UE is powered on, it connects to cell with the highest RSSI. As the UE moves, the serving cell  $RSSI_S$  is updated if the RSSI from the target SCeNB  $RSSI_T$  is higher than the RSSI of the serving cell  $RSSI_S$  plus handover hysteresis  $\Delta_{HM}$ , i.e. if

$$RSSI_T > RSSI_S + \Delta_{HM} \quad (3.1)$$

Courses of  $RSSI_S$  and  $RSSI_T$  are shown in Figure 3.7, as the UE moves in time and cell serving UE in each time is marked by a blue line.

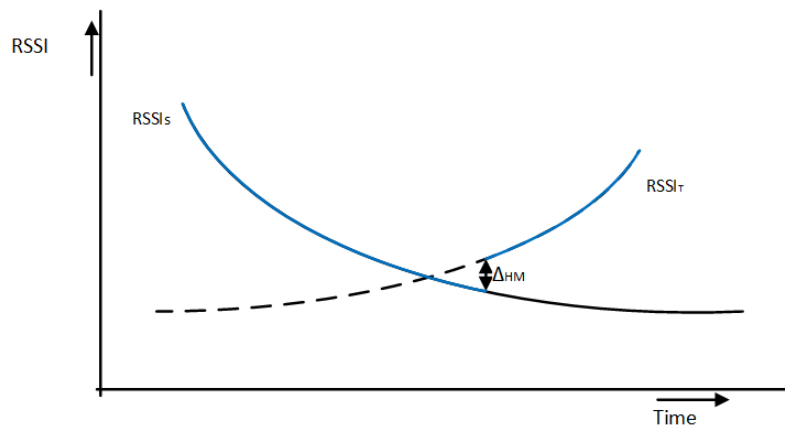


Figure 3.7: Basic handover procedure.

In networks with SCeNBs, handover can be executed in two ways as shown in Figure 3.8. Either using the X2 interface, where the source SCeNB hands over the UE to the target SCeNB (marked by the blue line) or by using the S1-signaling (marked by the yellow line) if direct forwarding is used (X2 interface is nonexistent or non-available) as in the most cases HeNBs are deployed by the users. Using the S1-signaling, the source SCeNB initiates handover procedure by sending message to the source MME, then the target MME is chosen. If the UE doesn't leave the source MME area, the source MME is also the target MME. However if the UE leaves the source MME area, new target MME and/or target SGW has to be chosen. If nothing blocks handover, the source SCeNB starts forwarding data to the target SCeNB. After data transfer is complete and SCeNBs have synchronized, the UE is handed to the target SCeNB [16].

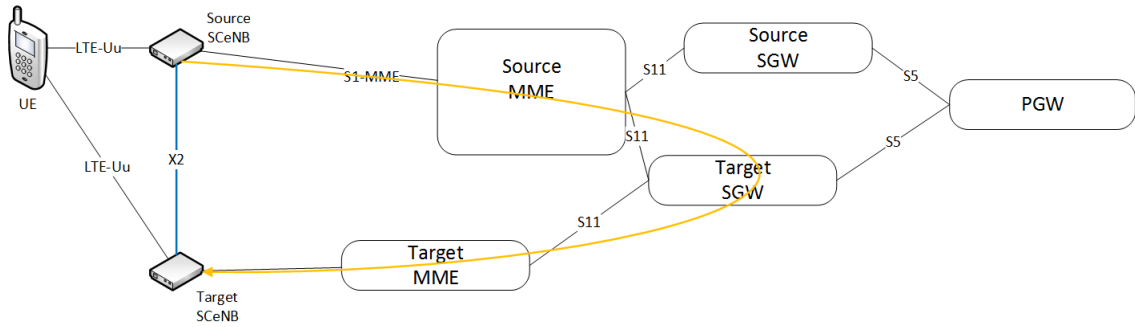


Figure 3.8: SCell handover variants.

### 3.3 Small cell cloud

In the SCC architecture, SCellNBs are further enhanced by storage and computing capabilities to provide cloud services of storing user data, caching data from the internet or processing applications such as facial recognition [24].

#### 3.3.1 SCC architecture

To provide cloud services, virtual machines (VM) are deployed over one or several SCellNBs, which form computing cluster. An architecture of cluster and its parts is shown in Figure 3.9. A hypervisor is the element that controls each VM on a given physical host system. The computing resources, the VM lifecycles, their start up, their states, and overall management of the SCC from the computing point of view is done by a Small cell Cloud Manager (SCM). The SCM is superior to hypervisors as hypervisor has knowledge only of the cell it controls, while the SCM is aware of all SCellNBs in the cluster.

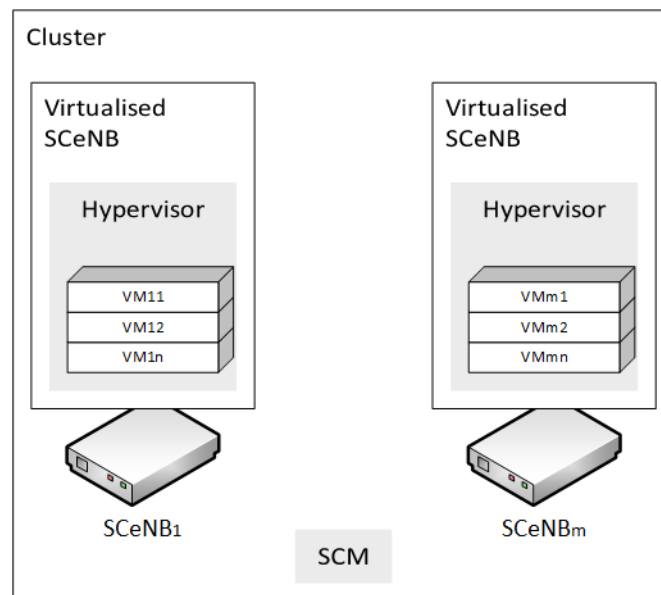


Figure 3.9: Cluster architecture.

### 3.3.2 Cloud request

Process flow of the UE creating SCC request and its processing shown in Figure 3.10 and has following steps :

1. The UE sends request through the serving SCeNB ( $SCeNB_{serving}$ ) to the SCM
2. The SCM decides whether offloading of request to the SCC is profitable. For the purposes of offloading decisions, the offloading module exists within SCM<sup>1</sup>.
3. The SCM sends reply whether offloading takes place [5] and which SCeNBs are used for offloading [25],[8]:
4. UE uploads data to the  $SCeNB_{serving}$
5. The  $SCeNB_{serving}$  takes out offloaded data designed to itself and starts processing, the rest of data is transmitted to other computing SCeNBs ( $SCeNB_1$  to  $SCeNB_n$ )
6.  $SCeNB_1$  to  $SCeNB_n$  receive data and process them
7.  $SCeNB_1$  to  $SCeNB_n$  transmit processed data back to the  $SCeNB_{serving}$
8.  $SCeNB_{serving}$  receives processed data from the other computing SCeNBs
9. Processed data are send back from the  $SCeNB_{serving}$  to the UE

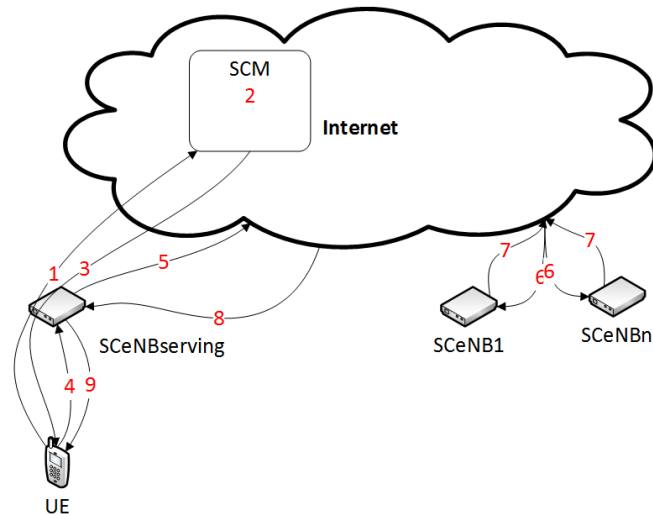


Figure 3.10: SCC request process.

<sup>1</sup>Decision whether to offload data to SCC are to be made by an offloading module, which resides at the SCM. Decision on offloading is based on the energy spend by the UE by execution of the request and by the latency and energy consumed by offloading request to the SCC [24]

### 3.3.3 Small cell cloud manager

The control and management of the SCC is in charge of the SCM. To define the SCM functionalities we divide them into a control plane and a user plane. The Control plane functionality comprise of those related to control and management policies such as VM and user management, monitoring, resource control and modification, etc. The user plane functionalities belong to those related to the user service delivery, such as application running and scheduling. The SCM is intended to receive UE messages through SCellBs as mentioned before. The SCM brings together radio and cloud to enable offloading to the SCC. Since the architecture of LTE-A has several variants and it is continuously evolving, various possibilities of placing SCM are considered:

- Placing the SCM as an extension of the HeNB-GW
- Deploying an In-cloud standalone SCM (provided that the coordination latency between SCM-SCellBs are concerned)
- The SCM as an extension of MME (if eNBs are considered)

All three above-mentioned options are described and analyzed in more details in [7].

# Proposed path selection algorithm for SCC

In this chapter, new path selection algorithm suitable for the SCC is proposed. In addition, a way how to obtain parameters required for the correct decision is also described. Last, complexity of the proposed solution is analyzed.

## 4.1 Path selection algorithm

In mobile networks, only path from the user to the computing cell through the serving cell is used. To overcome potential delay due to backhaul of limited throughput, arises an opportunity to use also neighboring cells and deliver individual parts of the data for computation to the specific computing cells through the cells, which offers lowest delay of the transmission over both radio and backhaul. Note that for each computing cell, data can be delivered through different serving cell. The proposed algorithm is named Path Selection with Handover (PSwH) and for the purposes of this thesis, existing scheme of using only serving is labeled Serving Only (SO).

The path selection algorithm suitable for the problem combines cost of data transmission over wired and wireless links with energy consumed by the UE for transmission over the radio in order to satisfy delay constraint  $T_{req}$ . Therefore, any delay higher than the required one is considered as unsuitable. If at least one available path fulfills  $T_{req}$ , all paths with delay exceeding  $T_{req}$  are dropped and are not considered in the path selection. If no path is able to provide delay lower than  $T_{req}$ , path with the lowest delay is selected.

The path selection is based on weighting of path delay ( $D$ ) and energy ( $E$ ) consumed by UE's transmission over the radio part of the path. In order to weight both metrics normalization is used as follows:

$$D_i^N = \frac{D_i}{\max(D_1, D_2, D_p)} \quad (4.1)$$

$$E_i^N = \frac{E_i}{\max(E_1, E_2, E_p)} \quad (4.2)$$

where  $D_i$  ( $E_i$ ) is the delay (energy) of the  $i$ -th path and  $p$  is the number of possible paths from the UE to the computing cell. The path selection is then defined as the Markov Decision Process (MDP), which calculates reward (penalty) of transition from the current state  $s$  to one of possible future states  $s'$  [26]:

$$V_\pi^k = Est[\sum_k R^t | \pi, s] = R(s) + \sum_k T(s, \pi(s, k), s') V_\pi^{k-1}(s') \quad (4.3)$$

$$\pi : s \rightarrow a \quad (4.4)$$



The current state  $s$  represents currently selected path (using the serving cell) and the future state  $s'$  represents another possible path including all combinations of radio and backhaul connections. Hence, the estimate ( $Est$ ) represents possible outcome of reward by performing handover to a different cell. The  $Est$  is computed over  $k$  steps, representing duration of the data transmission. Label  $\pi$  stands for the policy, which defines what action  $a$  should be taken in step  $s$  to maximize total reward as (4.4) denotes. Mapping an action  $a$  to a state  $s$  is a stationary policy if mapping is the same regardless of the time. Total reward for transition from the state  $s$  to the  $s'$  consists of two parts. The first one,  $R(s)$ , denotes immediate reward for transition from the state  $s$ . The second part, summation, represents expected future payoff as a sum over  $k$  steps. In this thesis,  $\pi$  is obtained at the end of the algorithm providing desired policy maximizing the reward. As delay and energy are used as metrics, optimal policies can be calculated in order to minimize delay, energy or both metrics. Reward depends on the delay due to handover if the handover is performed ( $T_H$ ), delay by the transmission over radio ( $T_R$ ) and delay on backhaul ( $T_B$ ). Thus, the reward for transition from the state  $s$  to the  $s'$  is written as:

$$V_{\pi}^k(s, s') = \gamma[k[E[T_R(s')] - E[T_R(s)]] + E[T_H(s, s')]] + (1 - \gamma)[T_H(s, s') + k[T_R(s') - T_R(s)] + k[T_B(s') - T_B(s)] \quad (4.5)$$

where  $\gamma$  is the weighting factor showing preference for low delay ( $\gamma=0$ ) or for high energy efficiency ( $\gamma=1$ ),  $E[T_R]$  denotes energy consumed by UE's radio communication through the serving cell (state  $s$ ) or another neighboring cell (state  $s'$ ),  $E[T_H(s, s')]$  stands for energy consumed by handover from the serving to the neighboring cell (from state  $s$  to state  $s'$ ). The transmission delays  $T_R$  and  $T_B$  are computed knowing amount of data to be transferred over radio ( $n_{bits}^R$ ) and backhaul ( $n_{bits}^B$ ) and knowing capacity of radio link ( $c_i^R$ ), capacity of backhaul of the serving ( $c_i^B$ ), and the computing ( $c_x^B$ ) cells:

$$T_R = \frac{n_{bits}^R}{c_i^R} \quad (4.6)$$

$$T_B = \frac{n_{bits}^B}{c_i^B} + \frac{n_{bits}^B}{c_x^B} \quad (4.7)$$

Each SCeNB can be powered off at any time since SCeNBs (HeNBs) can be deployed also by users who might turn device off. Thus, the problem of a link failure has to be addressed by keeping secondary path. To keep routing overhead low, in case of the link failure, data to be send over this link will be rerouted through the serving SCeNB if possible. In a case of the serving SCeNB failure, the UE will re-initiate path selection as there is major change in state of links, new path has to be calculated. Note that this problem requires also selection of new serving cell. However, this is common problem, for which even existing mobile network must be able to find a solution. Therefore, it is beyond the scope of this thesis.

## 4.2 Derivation of path selection parameters

To enable path selection, several metrics and information on several individual paths must be known. This subsection describes how the individual parameters can be derived in the existing networks.

The set of computing cells is labeled  $Y$ , the set of cells with radio access is denoted as  $I$ ,  $L_{UE}$  represents the load of data to be sent from the UE to computing cells and  $UE^i$  denotes  $i$ -th UE from the UE list. Parameter  $lambda$  specifies how to divide load into computing cells:

$$L_{UE} = \sum_{n \in Y} \lambda_n L_{UE} \quad (4.8)$$

$$\sum_{n \in Y} \lambda_n = 1 \quad (4.9)$$

While considering SCeNBs and especially HeNBs, the capacity of the radio link of the UE can be higher than the one of backhaul connection (especially for Digital Subscriber Line DSL). This leads to stress the importance of the radio link over the backhaul link with an exception of fiber optical or other high speed connection. In the proposed path selection algorithm, computation of metrics and routes is done at the SCM to lower energy consumption of the UE. In order to lower algorithm overhead and complexity NCL [17] is used. To describe the algorithm following notation of the sets of SCeNBs are introduced:

- $T$  - SCeNBs from NCL with SINR to UE above a selected threshold  $T_1$ :

$$T \subseteq I : SINR(T) \geq SINR_{T_1} \quad (4.10)$$

- $O$  - SCeNBs from  $T$  with SINR lower than UE has to serving SCeNB only by a selected threshold  $T_2$ :

$$O \subseteq T \quad (4.11)$$

$$SINR(O) \geq (SINR_{SCeNB_{serving}} - SINR_{(T_2)}) \quad (4.12)$$

These sets are made to lower the number of SCeNBs used to calculate optimal path. In  $T$  we remove SCeNBs to which the UE has SINR below the threshold value ( $T_1$ ) assure enough radio resources for data transmission. Since the UE uses the serving SCeNB there is no reason to make a handover to different SCeNB with SINR deep below ( $T_2$ ) SINR of its serving SCeNB. This way the  $O$  is created to cut off unusable SCeNBs with high delay from the algorithm and to reduce computational complexity of the proposed algorithm. These sets will be updated when there is a new SCeNB detected.

If a UE demands path to a single or multiple SCeNBs for its data :

1. The UE sends list  $T$  to its serving SCeNB and to all SCeNBs in  $O$
2. The serving SCeNB along with cells in  $O$  sends a new message to the cells in  $T$  to obtain delay and available bandwidth.

3. Using information obtained in the previous step, the serving SCeNB and SCeNBs in  $O$  derive their own routing tables with information on delay to the neighbors ( $T$  or  $Y$ )
4. The UE obtains cost of routes to computing SCeNBs and selects path with a minimal delay.

### 4.3 Management messages for exchange of the required information

For the path selection algorithm, two new management messages must be proposed to obtain information of delay and available bandwidth between each neighbor from the NCL with SINR above selected threshold. Format of both messages is shown in Figure 4.1. In order to use this technique, LTE in TDD version or LTE FDD with the network synchronization is required to obtain delay between two SCeNBs.

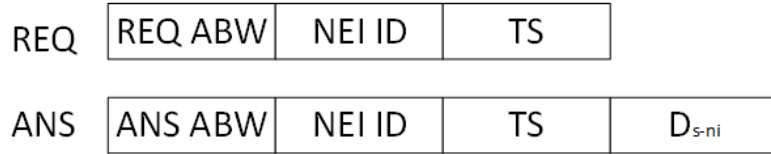


Figure 4.1: Message to obtain available bandwidth and measure delay.

1. Source SCeNB (i.e., the SCeNB requesting the information) sends **REQ** message to destination SCeNB (one of the neighbors). The **REQ** contains Request of Available Bandwidth (**REQ ABW**), Neighbor ID (**NEI ID**) and Time Stamp (**TS**).
2. Neighbor **ni** responds with **ANS** containing Answer with Available Bandwidth, its **NEI ID**, Time Stamp (**TS**) and delay observed for direction from the source cell to the neighbor  $D_{s-ni}$ .

$$D_{s-ni} = TS - receivedtime \quad (4.13)$$

3. The source SCeNB calculates backward delay from the neighbor to the source cell  $D_{ni-s}$  in the same way as the neighbor.

In the 3GPP specification [27] methods for obtaining packet delay measurement and Scheduled IP Throughput for the radio part are described. Packet delay is intended for use of Voice over IP (VoIP) and thus downlink and uplink are measured independently. Measurement uses same principle of sending time stamp and calculating delay from subtracting two values. Difference is in calculation of delay for donwlink and uplink separately. IP throughput is measured for LTE-uU interface which serves for control transmissions with MME and also data transmission with S-GW both being realized utilizing SCeNB. For the use of PsWH methods from [27] can be used on the radio link (LTE-A), while the proposed message needs to be implemented in order to calculade backhaul delay and to obtain available bandwidth so SCM can chose optimal path.

## 4.4 Algorithm complexity

Complexity of the path selection algorithm is proportional to the number of computing SCeNBs ( $n$ ) and the number of SCeNBs in proximity of the UE ( $m$ ). The SCeNBs in proximity of the UE are selected according to the SINR. Number of possible paths can be computed as partial permutation thus complexity of the proposed path selection algorithm is  $O(m^n)$ .

# System model and simulation methodology

In this section, models and scenarios for performance evaluation are defined. The evaluation is carried out by means of simulations in the MATLAB.

## 5.1 System model

The system model is assumed to be composed of  $S$  SCeNB and  $U$  UEs and the selection of serving cell is following scheme from the 3.2.1 on page 8.

For each computation offloading request, the maximal delay of data delivery from the UE to the computing cells,  $T_{req}$ , is specified. This delay can be derived as a difference between maximum delay required by the UE for delivery of the computation results back to the UE ( $T_{max}$ ) and the time required for computation of the offloaded task ( $T_{comp}$ );  $T_{req} = T_{max} - T_{comp}$ . Parameters  $T_{max}$  and  $T_{comp}$  are related to application and available computing capacity of cloud-enhanced SCeNBs, respectively. For purposes of PswH, specific way of  $T_{max}$  and  $T_{comp}$  derivation is not relevant; it just needs to know the time constraint remaining for data transmission.

The set of SCeNBs selected for computation is denoted as a  $Y$ . Each cell is expected to compute a part  $\lambda_n \in (0, 1]$  of the whole offloaded task of the overall size of  $L_{UE}$ . The individual part  $L_n$  computed by the  $SCeNB_n$  is then expressed as  $L_n = \lambda_n L_{UE}$  with  $\sum \lambda_n = 1$ . In this thesis, equal distribution of the task among all computing cells i.e.  $\lambda_1 = \lambda_2 = \dots = \lambda_n$  is assumed.

As shown in Figure 5.1, data from the  $UE$  to the  $SCeNB_i$  is transferred over radio link with capacity  $c_i^R$ . Further, the  $SCeNB_i$  is connected to the operator's core with a backhaul of capacity  $c_i^B$ . Data is then processed by the  $SCeNB_i$  or forwarded to another computing  $SCeNB_x$  through backhaul of the  $SCeNB_i$  (with capacity in uplink) and backhaul of the computing cell  $SCeNB_x$  (with capacity  $c_x^B$  in downlink). Note that index  $x$  stand for any SCeNB out of  $S$  except  $SCeNB_i$ . After cells perform data computation, the results are delivered back to the  $UE$ . New path for backward data delivery (from  $SCeNB_x$  to the  $UE$ ) can be derived if radio and backhaul links are not symmetric in uplink and downlink, if the UE moves during computation or if the channel/link load or quality change. Otherwise, the same path can be reused.

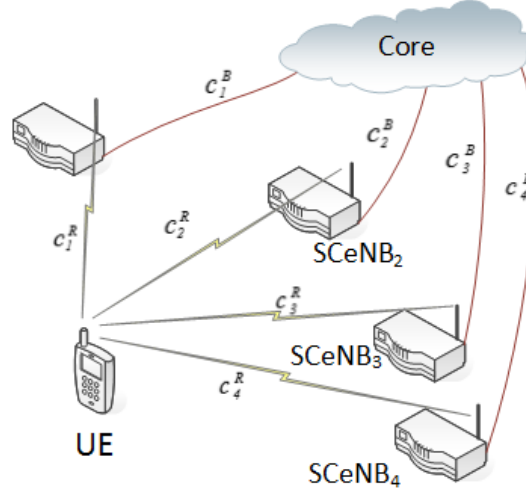


Figure 5.1: SCC system model.

### 5.1.1 Transmission of offloaded data

In an uplink connection as in LTE-A SC-FDMA is used, as a way to transmit to different SCeNB, handover needs to occur. While in Wideband Code Division Multiple Access (WCDMA) networks possibility of the soft handover existed, in LTE and LTE-A there is only hard handover. If UE transmits data to the computing SCeNB  $Y_1$  and multiple SCeNBs are being used to compute data. Handover (on a radio interface) to other computing SCeNB  $Y_2$  should occur only if the delay to deliver required data utilizing radio connection to  $Y_2$  and delay caused by a handover is lower than the delay utilizing radio to  $Y_1$  and backbone connection between  $Y_1$  and  $Y_2$  as follows:

$$D_{Y_1 radio} + D_{Y_2 backhaul} > D_{Y_2 radio} + D_{handover to Y_2} \quad (5.1)$$

To illustrate how much data can be transmitted on a radio interface of LTE during the handover (30 ms) procedure is shown below in a Figure 5.2.

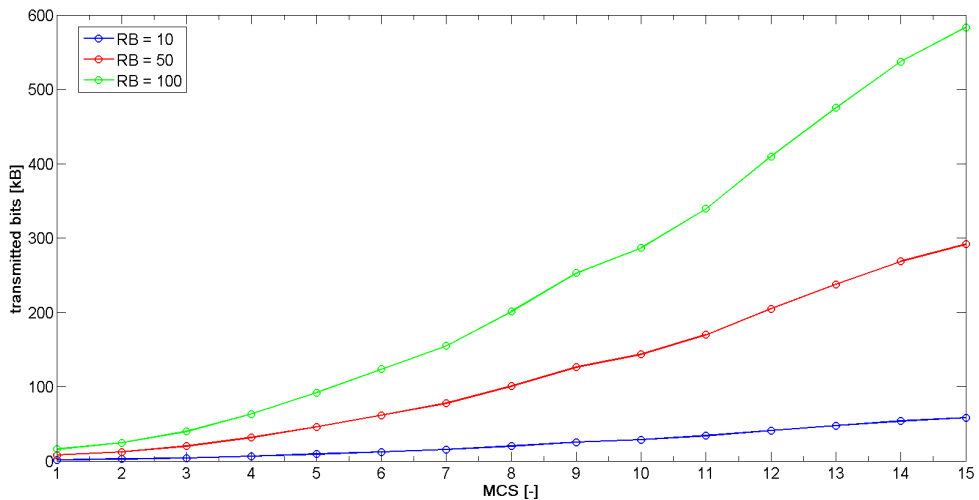


Figure 5.2: Unused bits for handover duration 30 ms.

## 5.2 Simulation scenario and models

Major parameters of the simulation, presented in Table 5.2 are in line with the recommendations for networks with small cells as defined by 3GPP in [28]. We also follow parameters of the physical layer and frame structure for the LTE-A mobile networks as defined in the same document.

For the simulation purposes two approaches differing in the point of view are investigated:

- UE point of view
- Network point of view

In the UE point of view, direct comparison of the SO and the PSwH is made. From this point of view can show, how the PSwH leads against the SO if UE makes request for the path. In this simulation, both algorithms are compared side by side, meaning in the same network states (same amount of resources on the radio and the backhaul is available). As for the radio we use Guaranteed Bit ratio (GBR) [29], which tries to provide minimal Quality of Service (QoS) by allocating minimal specified amount of bit rate for the UE. For the purpose of the comparison, we reserve 10 RBs for the each request. As for the backhaul, UEs requests data transmissions are not affecting network load as this would not allow to compare algorithms in the same situations. From this scenario optimal policies for the UE depending on its requirements can be obtained.

Second scenario focusing on the network point of view, however utilize effect of generated requests on the network state in order to compare which one is better from the network resource usage. For this scenario, two options of radio connection sharing are used. First one uses the same GBR principle and the second one shares resources between requests in a manner, that newly incoming requests are given less resources as we reserve part of the resources for the requests to come. From this scenario, optimal policies for the network (meant as what is the best from the network point of view) can be obtained.

Signal propagation is modeled according to 3GPP [29]. Depending on the location of UE and its serving cell (eNB or HeNB), one of the path loss models from [30] is used. In Table 5.2 are shown losses due to wall attenuation. Two-dimensional correlated shadowing model with temporal time correlation [31] is used as well.

Based on the path loss, the throughput of UE is derived using a mapping function for the SINR and the MCS as obtained from [32] with block error rate of 10 % (see 8.2). The MCS is then used for computation of radio link capacity. For this we assume allocation of 10 RBs for each user demanding the SCC services. Furthermore, we assume 20 RBs are consumed by background traffic generated by users not exploiting the SCC. For the simulation purposes, backhaul models as DSL and optical fiber are used since these are the most common backhaul connection for residential and office users. For the each SCeNB, the capacity of backhaul is selected using uniform discrete distribution with parameters from Table 5.2 .

Requests for data offloading are generated by UEs continuously, just after end of the previous one, to model behavior of heavily loaded system. This case is the most challenging due to limited capacity of backhaul and radio. Each request corresponds to the generated traffic of 300kB and 30 MB for the UE point of view and to 300 kB

and 3 MB for the network point of view. The offloaded data is computed at 2, 3 or 4 cells, with equal probability of each option. One of the computing cells is always the serving one (as suggested in [9]).

All UEs are moving within an area composed of two-strips of buildings [28] as shown in Figure 5.3. Size of each block of buildings is 20x100m and blocks are separated by streets with width of 10m. The overall area is composed of 4x4 blocks (i.e., size of the whole simulated area is 560x130m). Fifty outdoor UEs are randomly deployed at the beginning of the simulation and then they move along the streets according to Manhattan Mobility model [33], with movement speed of 1 m/s.

Besides SCeNBs also an eNB is placed outside the area with the two stripes buildings at coordinates of [200m, 200m]. In simulation three types of computing SCeNBs selections are used: random selection of  $n_{computing}$  SCeNBs from the  $n$ -closest, and determined number of computing SCeNBs (1,2,3,4).

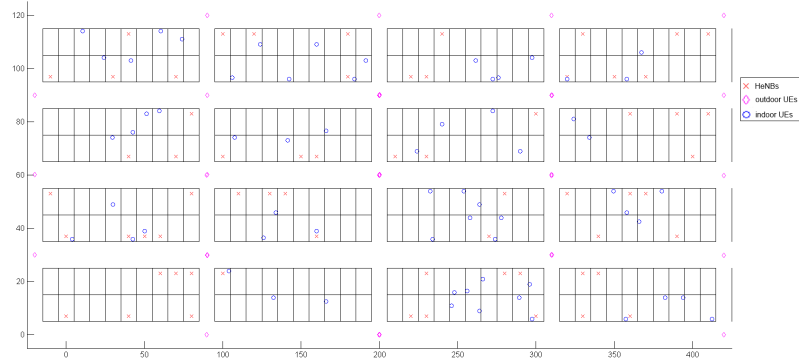


Figure 5.3: Simulation area.

Inside of buildings, the SCeNBs are randomly dropped to the apartments with equal probability in a way that 20% of apartments are equipped with a SCeNB. Therefore, 80 UEs and 80 SCeNBs are deployed indoor. Movement of the indoor UEs is modeled according to [30] and show in Figure 5.4, i.e., the UEs move within an apartment at discrete positions with time distributions from [34].

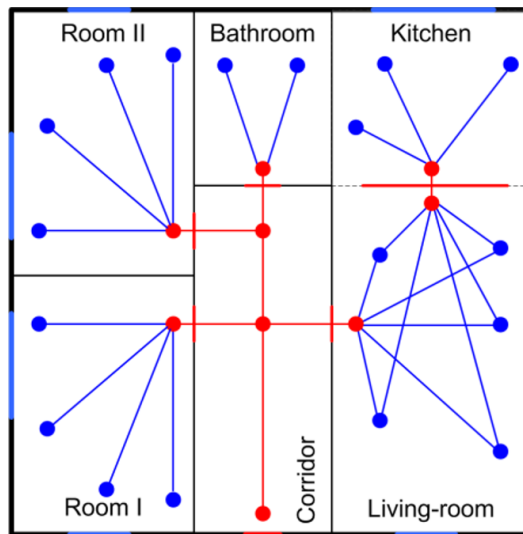


Figure 5.4: Indoor movement.



The UEs stays for a given time at the positions of stay marked by blue dots in Figure 5.4. Time spent by the indoor UE in each spot is given by distributions and their parameters as defined in Table 3 [30]. Movement among the points of stay is through temporal positions (marked as red dots).

Table 5.1: Distribution of time stay in specific rooms for indoor movement

Room	Distribution and its parameters
Room I, room II, and living-room	Normal, $\mu = 1800$ , $\sigma = 150$
Kitchen	Normal, $\mu = 1200$ , $\sigma = 150$
Bathroom	Normal, $\mu = 300$ , $\sigma = 22$
Corridor	Normal, $\mu = 80$ , $\sigma = 22$

Table 5.2: Simulation parameters

Simulation area	560 m x 130 m
Carrier frequency	2000 MHz
Tx power of eNB/SCeNB [dB]	43/23
Attenuation of external/internal/separating wall [dB]	20/3/7
ScNB deployment ratio	0.2
Shadowing factor [dB]	6
Handover duration [ms]	20/500
Number of Indoor/Outdoor UEs	64/50
Speed of outdoor users	1 m/s
Traffic generated by one request [kB]	30/30000
Simulation time	5 000s

In order to show how proposed algorithm works, two types of backhauls are used. The first one is the Residential, in this model, SCeNBs are deployed at private flats within the same building. As the typical backhaul connection of each flat is the DSL. The second model is Corporate with fiber optic backhaul and Local Area Network (LAN) consisting of Ethernet connection with the throughput of 100 Mbit/s as specified in Table 5.3, as better backhaul connections are used in work offices. In addition, interconnection of SCeNBs within the same block is used as they are likely to be interconnected through company LAN connection. In a case when two or more SCeNBs from the same block communicate we use this LAN connection instead the shared connection to the internet.

### 5.2.1 Energy consumption model

With the effort of the SCC to extend UE battery life, by offloading computing load, we use LTE-A radio power models the second metric. Being it smartphone, tablet or 3G USB module each device essentially has to produce same radio out specified in standards. From the standards [14] and models from [2], [35] and [36] we calculate power requirements on the UE, based on received signal, required throughput, etc. The energy  $E$  is computed as the power consumed by the UE for data transmission over a transmission time. Since both uplink and downlink power models are different, we describe them separately. As the communication structure is the same for the both directions, both are shown in Figure 5.5.

Table 5.3: Backhaul parameters

<b>Corporate model (optical fiber)</b>	
$\mu$ (backhaul UL/DL)	100/100 Mbit/s
$\sigma$ (backhaul UL/DL)	11.5/11.5
Shared block backhaul UL/DL	100/100 Mbit/s
eNB UL/DL	1000/1000 Mbit/s
<b>Residential model (ADSL)</b>	
$\mu$ (backhaul UL/DL)	1/5.5 Mbit/s
$\sigma$ (backhaul UL/DL)	0.52/2.6
eNB UL/DL	1000/1000 Mbit/s

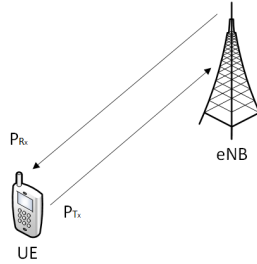


Figure 5.5: UE to eNB communication.

## Uplink

In the uplink, meant as from the UE (transmitter) to SCeNB (receiver) are data transmitted using Physical Uplink Shared Channel (PUSCH). The energy consumption of the uplink depends on the Modulation and Coding Scheme (MCS) and available bandwidth represented by Resource Blocks (RBs) in the LTE-A system. The MCS is a function of the SINR observed at the receiver. The SINR at the receiver is proportional to transmission power  $P_{Tx}$  at transmitter, path loss and interference from other cells. In LTE, the  $P_{Tx}$  required for selected MCS for a given number of allocated RBs is defined, according to 3GPP [14] and [35], as follows:

$$P_{Tx} = \min(P_{MAX}, P_0 + \alpha PL + 10 \log_{10}(M) + \Delta_{TF} + f [mW]) \quad (5.2)$$

where  $P_{MAX}$  is the maximum available transmission power (23 dBm or the UE class 3 [3]);  $\alpha \in 0, 0.4, 0.5, 0.6, 0.7, 0.8, 0.9, 1$  corresponds to the path loss compensation factor,  $PL$  is the downlink path loss estimate,  $M$  stands for the number of assigned RBs,  $\Delta_{TF}$ , where  $TF$  stands for Transport Format (TF), represents a closed loop UE specific parameter, which is based on the applied MCS, and  $f$  is a correction value, also referred to as a Transmitter Power Control (TPC) command. (more details on  $\Delta_{TF}$  and  $f$  are found in [14]); and parameter  $P_0$  represents the power offset computed as:

$$P_0 = \alpha(SINR_0 + P_N) + (1 - \alpha)(P_{MAX} - 10 \log_{10}(M_0) [mW]) \quad (5.3)$$

where  $P_N$  is the noise power per RB computed as:

$$P_N = -174 + 10 \log_{10}(M) [dB] \quad (5.4)$$

and  $M_0$  defines the number of RBs for which the  $SINR_0$  is set with full power.

Parameters  $\Delta_{TF}$  and  $f$  are used for dynamic adjustment of the transmission power to keep required SINR at the receiver. There are two existing power control schemes used to compensate effects of path loss, shadowing, fast fading and implementation loss. For the power control schemes, eNB transmits necessary power control information through the transmission of power control messages. Each eNB optimizes these parameters to desired goal of the operator as by use of the power control parameters can be set in a way that the edge users will be preferred or we prefer system throughput and thus closest users. The closed-loop power control allows UE to adapt the uplink transmit power according to the closed-loop correction values received from the eNB (mentioned TPC commands). The TPC commands are transmitted from the eNB to the UE, based on the closed-loop target SINR and the measured SINR. When the received SINR is below the target SINR, a TPC command is transmitted to the UE to increase the  $P_{TX}$ . If the target SINR is above the measured SINR, TPC command to decrease the  $P_{TX}$  is transmitted to the UE. The second approach for power control is named open-loop, which is not using measured data from eNB to adjust transmission power and rather depends on measurement of UE only as is shown in Figure 5.5.

As open loop is used in this thesis as a power control, TPC parameters can be omit as indicated in [37] or proposed in [[2] to obtain UE initial power by ignoring them. The parameter  $\alpha$  is set to 1 so the UE fully compensates path loss. Under these assumptions, power offset can be simplified to:

$$P_0 = \alpha(SINR_0 + P_N)[mW] \quad (5.5)$$

and then, 5.5 can be rewritten as:

$$P_{Tx} = \min(P_{MAX}, \alpha(SINR + P_N + PL) + 10\log_{10}(M))[mW] \quad (5.6)$$

The energy consumed by transmission of data over a radio is derived, according to [35] as:

$$E = P_{Tx}T_R[J] \quad (5.7)$$

An example of the tradeoff between energy and time of a transmission of 100 kB using 10 RBs with  $PL=80$  dB for different MCS is shown in Figure 5.6. As this figure shows, high energy is consumed by transmission of short duration. Contrary, less energy is consumed for higher transmission time. From the figure it can be concluded that using high MCS is not energy efficient and if there is no delay constrain or constraint would be satisfied by using lower MCS, UE energy can be saved as it would require lower transmission power.

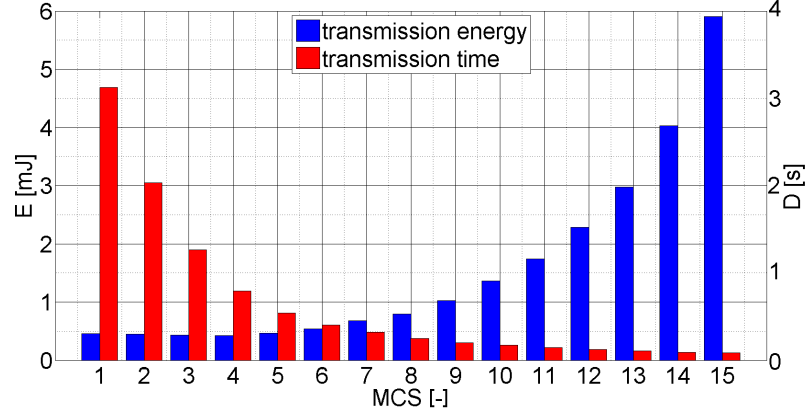


Figure 5.6: Example of energy consumption ( $PL = 80dB$ ,  $10RBs$ ,  $100kB$ ) transmission.

### Downlink

For the energy consumed by the UE in the downlink direction, different model is used. Power required to process receiving data depends on  $P_{rx}$  and data rate as well. Main power consuming part of the UE is the power amplifier and the turbo decoder. In this thesis, power consumption model from [36] is used to match power consumption to data transmission while we have  $P_{rx}$  and data rate, using following:

$$P_{RxRF} = \begin{cases} -0.04S_{Rx} + 24.8[mW] & S_{Rx} \leq -52.5dBm \\ -0.11S_{Rx} + 7.86[mW] & S_{Rx} \geq -52.5dBm \end{cases}$$

$$P_{RxBB} = 0.97R_{Rx} + 8.16[mW] \quad (5.8)$$

$$P_{Rx} = P_{RxRF} + P_{RxBB}[mW] \quad (5.9)$$

where  $P_{RxRF}$  denotes radio component depending on the received power  $S_{Rx}$ ,  $P_{RxBB}$  denotes radio component depending on bit rate of received transmission. Since at  $S_{Rx} = -52.5dBm$  power amplifier is switched to different, so the used power amplifier works within linear area. Energy consumption is calculated using equation (5.7) as used in the uplink. How much power is required by receiving transmission is shown in Figure 5.7. Course of power consumption is linear apart from the part where switching of power amplifiers occurs. From the model it can be derived, that it is best to use bit rate as high as possible as there is less than linear increase in power consumption with linear increase in bit rate.

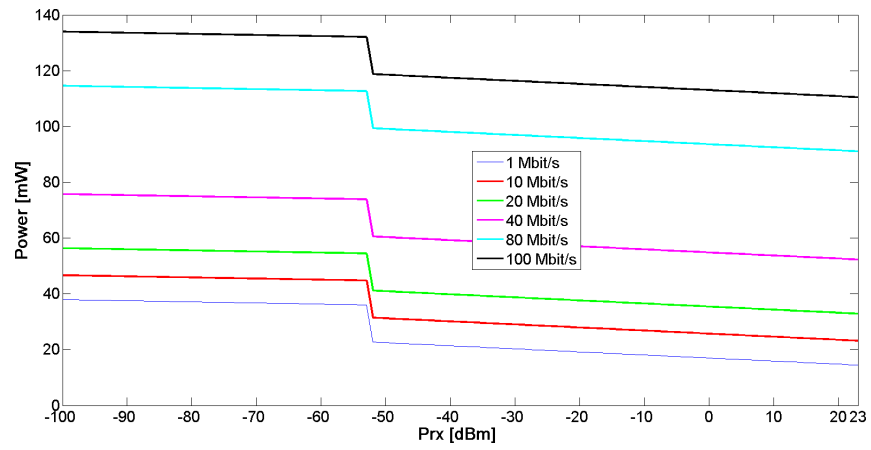


Figure 5.7: Downlink power consumption.

# Simulation results

In simulations, comparison of the proposed path selection with handovers (PSwH) against conventional algorithm, which transfers data to all computing SCellNBs through the serving SCellNB [7]. In this thesis this algorithm is denoted as Serving Only (SO). Comparison of results is done by comparing UE satisfaction, mean  $D$  and  $E$  spent by data transmission over the selected path using the SO and the proposed PSwH.

## 6.1 UE point of view

In this part, simulation to compare the PSwH against the SO from the UE point of view is evaluated. Both algorithms calculate path for the same network situation (radio and backhaul have same amount of free resources).

Impact of the proposed PSwH algorithm on average delay of offloaded data transmission between the UE and computing SCellNBs is depicted in Figures 6.1 and 6.2. As can be seen, the delay is shortened more significantly for backhaul with limited capacity (DSL). For DSL, the proposed PSwH reduces delay between 9% if delay is preferred ( $\gamma = 0$ ) and 2% if energy consumption is more important ( $\gamma = 1$ ). This ratio is nearly independent on the amount of data to be transferred per request for computation offloading as shown in Figure 6.1 and 6.2. If the backhaul of higher capacity is considered (in our case, optical fiber), the gain is lower (4.7% and 4.0% for  $\gamma = 0$  and  $\gamma = 1$ , respectively) because this backhaul is able to forward data to the computing cell in a shorter time and handover is not efficient in this case.

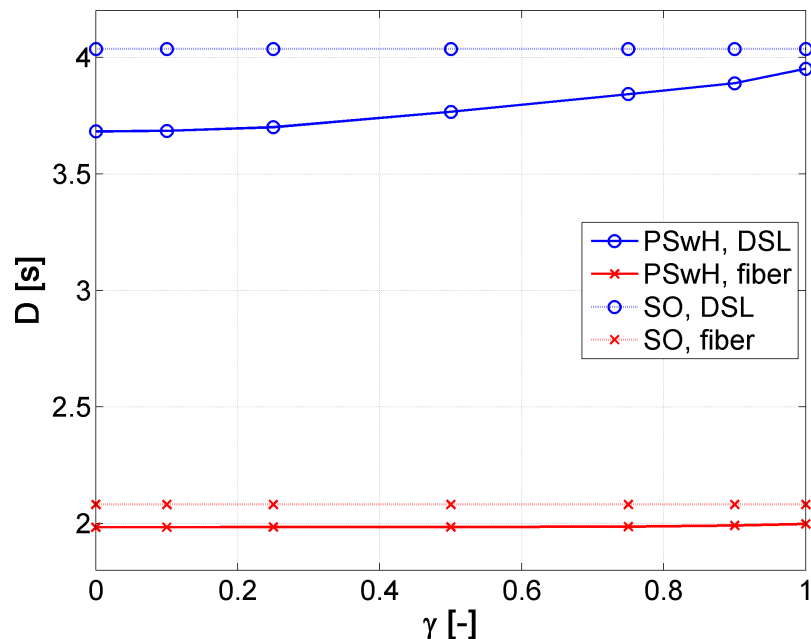


Figure 6.1: Average delay  $D$  required for transmission of offloaded computing task to computing cells for request size of 300kB.

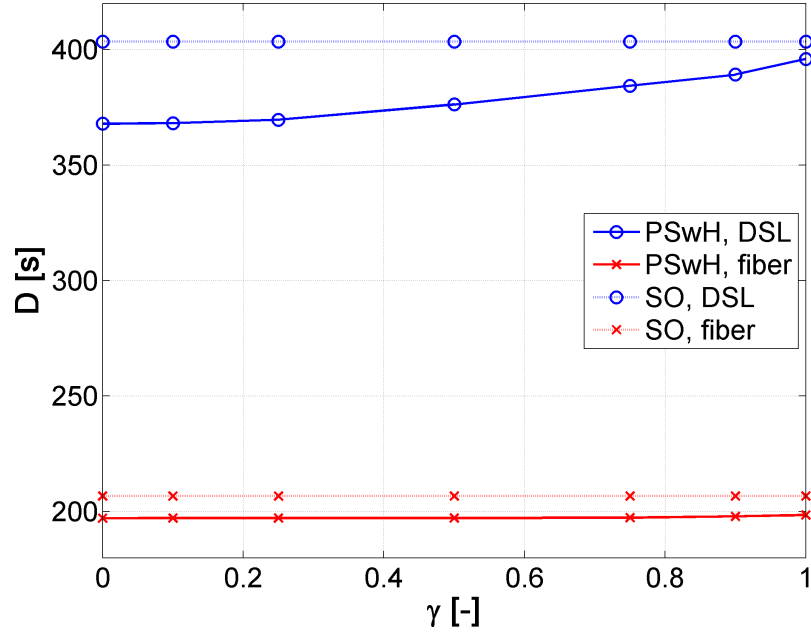


Figure 6.2: Average delay  $D$  required for transmission of offloaded computing task to computing cells for request size of 30 MB.

The proposed PSwH should avoid dramatic draining of the UE's battery due to handover. In Figure 6.3, is shown that the energy consumption of the PSwH is similar as for the SO if optical fiber is used for backhaul and if each request is of 300kB (PSwH reduces  $E$  by 0.2%). If the amount of transmitted data is increased to 30MB (Figure 6.4), energy consumption is slightly increased by the PSwH (by 1.9%) if delay is preferred ( $\gamma = 0$ ). However, for  $\gamma \geq 0.1$ , the energy consumption of both is roughly the same for optical fiber backhaul (the PSwH even negligibly outperforms the SO by 0.2%). For DSL backhaul, the PSwH requires more energy comparing to the SO for low  $\gamma$  (approximately 5.5% if  $\gamma = 0$ ). This is due to selection of worse radio channel, which is less energy efficient, in order to avoid backhaul with limited capacity. Nevertheless, by setting  $\gamma = 0.5$ , energy consumption of the PSwH is again the same as for the SO.

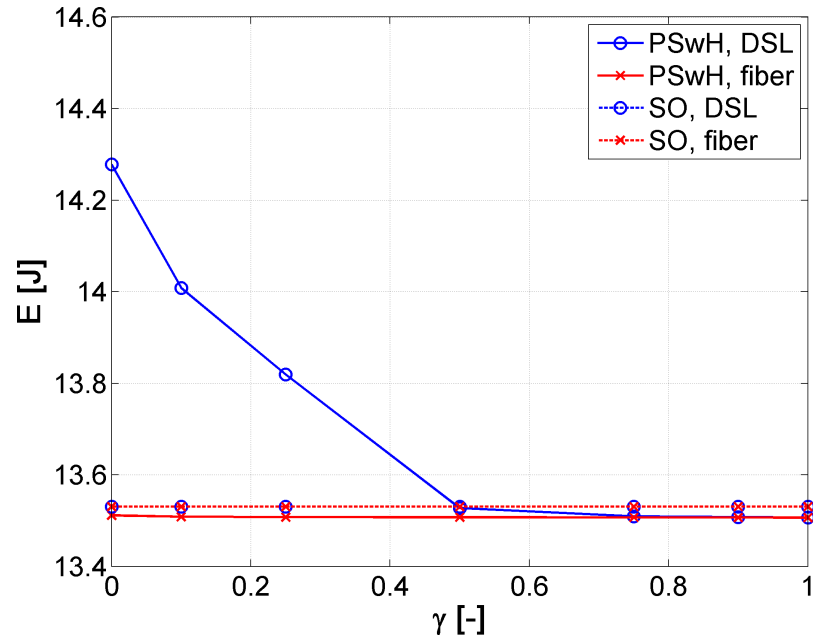


Figure 6.3: Average energy  $E$  consumed by radio transmission of offloaded computing task to computing cells for request size of 300kB.

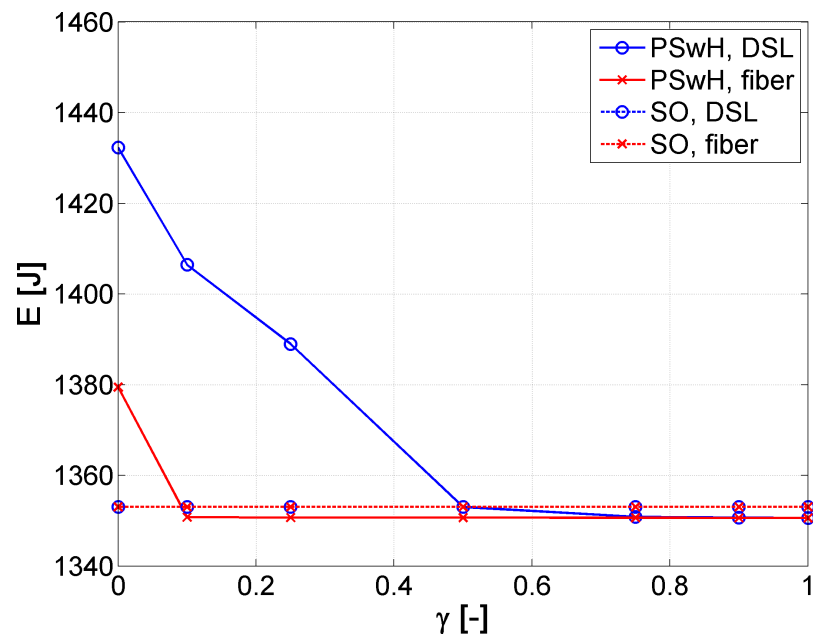


Figure 6.4: Average energy  $E$  consumed by radio transmission of offloaded computing task to computing cells for request size of 30 MB.

From above discussion, conclusion can be made that the PSwH enables to reduce delay by 9% and 4.7% if  $\gamma = 0$  for DSL and optical fiber backhails, respectively. This is at the cost of higher energy consumption (increased by 5.5% for DSL and 1.9% for optical fiber). However, by setting  $\gamma = 0.5$  for the PSwH if DSL is used, delay can be shortened by 6.7% while energy consumption is also reduced by 0.2%. For optical fiber backhaul, the most efficient is to set  $\gamma = 0.1$ , which results in shortening the delay by 4.7% and energy consumption reduction by 0.2%



The satisfaction of UEs using the PSwH and SO algorithms is shown in Figure 6.5 (for offloading of 300kB) and Figure 6.6 (for offloading of 30MB). The satisfaction is understood as the ratio of users, whose experienced delay is not higher than the requested one (i.e.,  $D \leq T_{req}$ ). As can be seen from Figure 6.5 and Figure 6.6, the UE's satisfaction is increasing with  $T_{req}$  for both algorithms. This fact can be expected as with higher  $T_{req}$ , more time is available for delivery of data. Comparing the PSwH with the SO, the proposed algorithm increases the satisfaction up to 6.5% for DSL backhaul and for both amounts of offloaded data (300kB as well as 30 MB). The satisfaction increases as  $\gamma$  decreases because more stress is put on delay in this case while energy is less important. For optical fiber backhaul, the PSwH improves the satisfaction by 2.8% and by 1.8% for 300kB and 30MB size of requests, respectively. The lower improvement in satisfaction for optical fiber backhaul and lower size of offloaded data is due to the fact that high capacity backhaul can easily transfer requests of small size from the serving cell to the computing cells and handover to computing cells is not necessary.

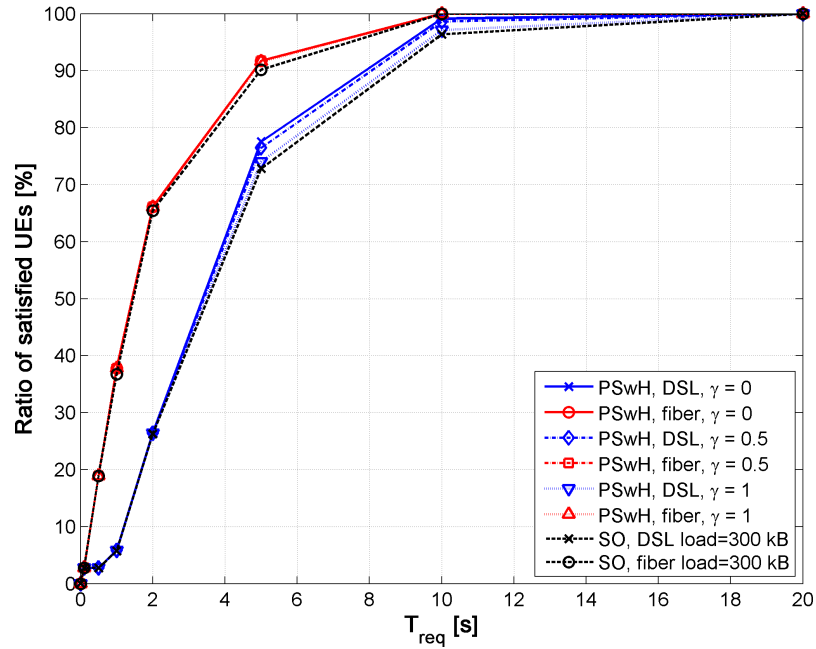


Figure 6.5: Satisfaction of users with experienced delay for request size of 300 kB.

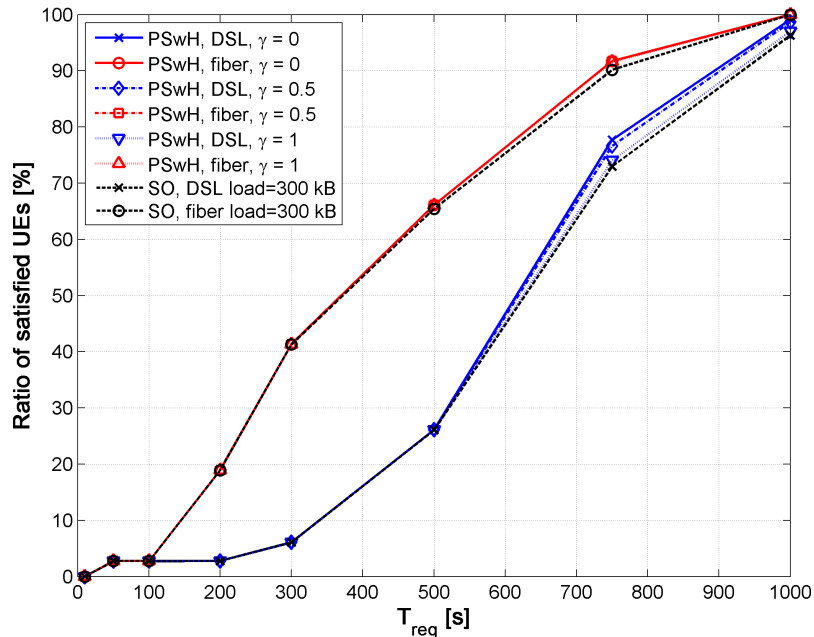


Figure 6.6: Satisfaction of users with experienced delay for request size of 30 MB.

The proposed algorithm introduces additional handovers, which can lead to handover interruption and redundant signaling. The first problem, handover interruption, is not related to the SCC services as the users do not care about interruption in data transmission, they insist on the overall delay of computing results delivery. Impact of the handover interruption on the overall delay is considered in the PSwH (see 4.1), thus all results already consider this issue.

For analysis of impact of handover on the signaling overhead, average increase in amount of handovers performed by users is shown in Figure 6.7. From this figure, we can observe that the number of additional handovers is higher for DSL backhaul if preference is set to experience low delay ( $\gamma = 0$ ). With respect to usage of the SO algorithm, additional 20% of handovers are performed. In this case, transferring data over backhaul with low capacity requires more time and, consequently, it is more difficult to meet  $T_{req}$ . Therefore, performing handover to a computing cell is more often as the UE can use radio of a higher quality instead of low quality backhaul for data transfer. Nevertheless, with preference for low energy consumption ( $\gamma = 1$ ), the users stick to the serving cell providing mostly the highest channel quality and thus it is the most energy efficient. In this case, increase of only 7% in number of handovers is observed.

For optical fiber backhaul, the number of additional handovers converges to 7% with  $\gamma = 1$  for both amounts of data transferred per request. Nevertheless, for  $\gamma = 0$ , the request of small size (300 kB) is transferred over backhaul so promptly that time consumed by handover itself is more significant. Hence, handover is performed less often. Generated overhead due to handover is in order of kb per handover event [38]. Consequently, considering the results presented in Figure 6.7, we can conclude that increasing number of handover by 20% leads to negligible increase in signaling overhead due to handover management.

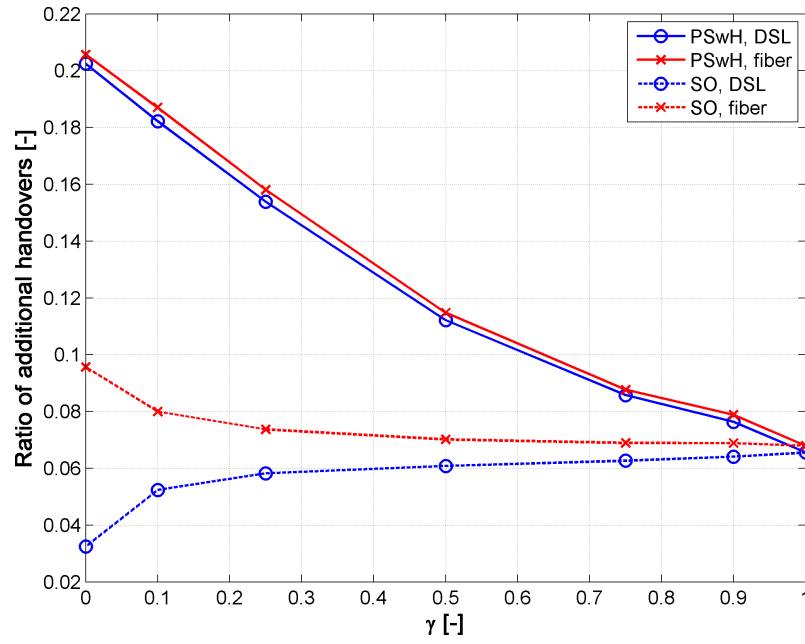


Figure 6.7: Ratio of additional handovers due to proposed algorithm with respect to usage of serving cell only (SO).

Effect of the number of computing SCeNBs, as a gain in delay is shown in Figure 6.8 and 6.9. As we can see as the number of computing SCeNB increases, PsWH provides higher gain in delay up to the 9% when there are 4 computing SCeNBs for the DSL backhaul and up to 8.2% when optical fiber is used.

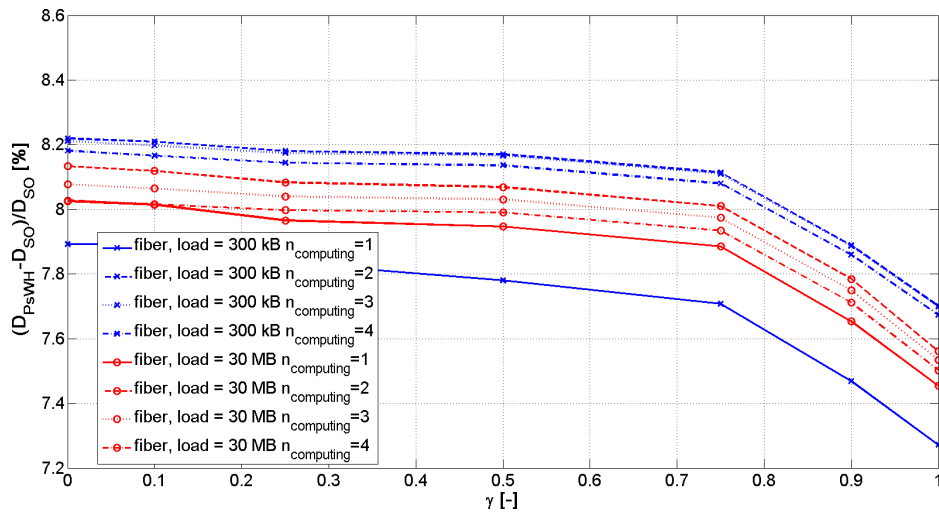


Figure 6.8: Gain in delay against SO for optical fiber backhaul.

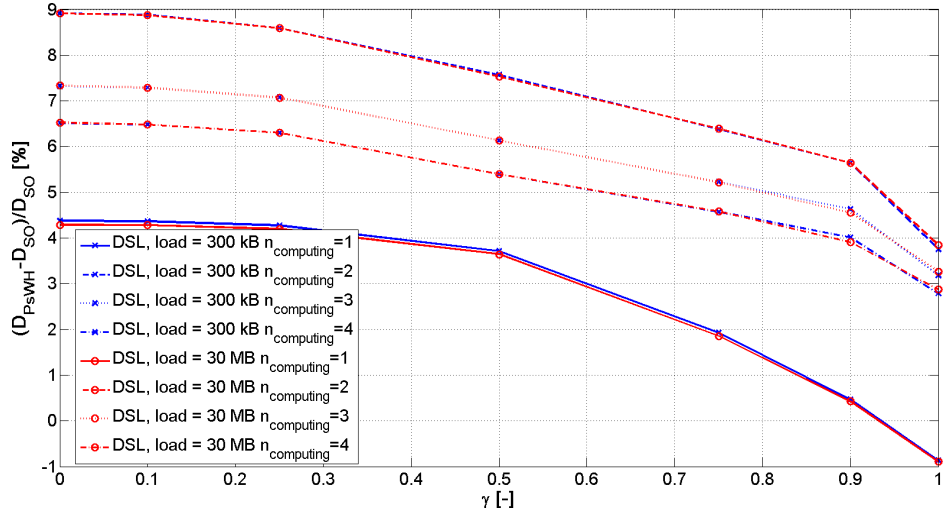


Figure 6.9: Gain in delay against SO for DSL backhaul.

As delay gain is compared, comparison of gain in  $E$  against SO is shown in Figures 6.10 and 6.11. For optical fiber, when load of 30 MB is required, increase of required energy  $E$ , for  $\gamma < 0.1$  is seen, but as  $\gamma > 0.1$ , the PsWH provides 0.6 % gain in energy for both requests load. If DSL is used as a backhaul, increase in required energy is seen as the number of computing SCeNB increases. However as  $\gamma$  reaches 0.5, the PsWH requires same energy for the load data transmission.

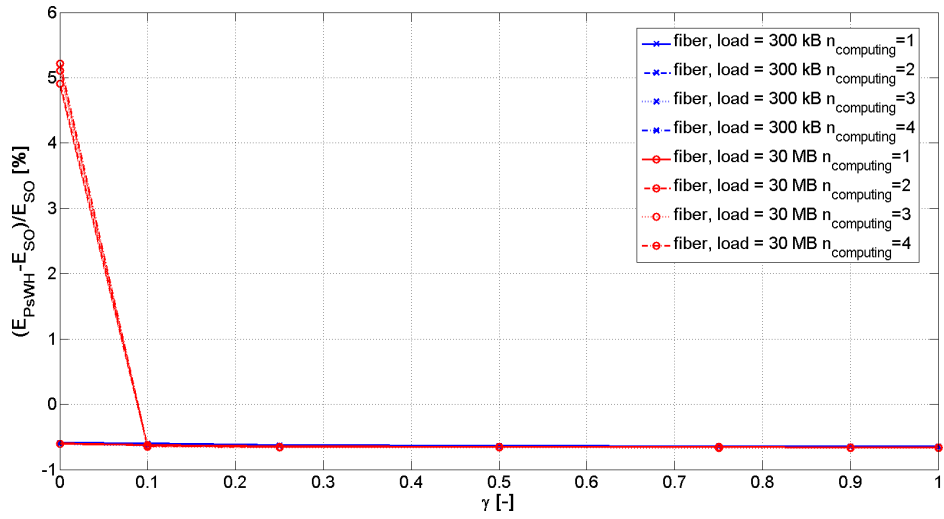


Figure 6.10: Gain in energy against SO optical fiber backhaul.

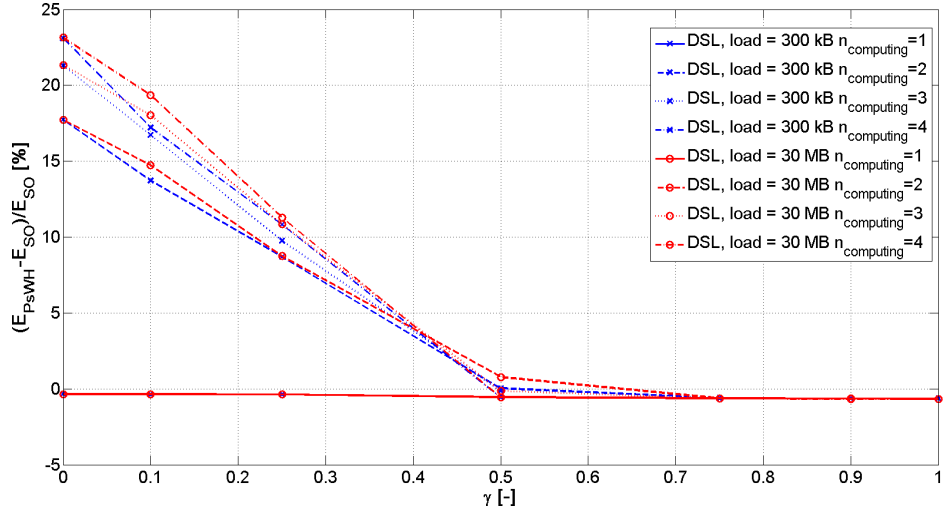


Figure 6.11: Gain in energy against SO DSL backhaul.

## 6.2 Network point of view

For the network point of view scenario parameters of time between two requests ( $T_{\text{betweenreq}}$ ) and two requests from the same UE ( $T_{\text{UEreq}}$ ) in network and between two requests from one user, had to be derived in order to not overload the network. By experimental measurement we obtained  $T_{\text{betweenreq}}=2$  s and  $T_{\text{UEreq}}=128$  s, when 300 kB requests are generated. If UE generates requests of 3 MB,  $T_{\text{betweenreq}}$  is increased to 15 s and  $T_{\text{UEreq}}$  to the 960 s.

### 6.2.1 GBR

In this part, each request on radio has GBR of 10 RBs and backhaul connections are shared.

In comparison of delay, in Figure 6.12 for 300 kB, the PSwH brings almost zero improvement, however if the request load is 3 MB, the PSwH starts to provide up to 400 % lower delay in case of DSL and up to 500% lower delay in case of the fiber backhaul as shown in Figure 6.13.

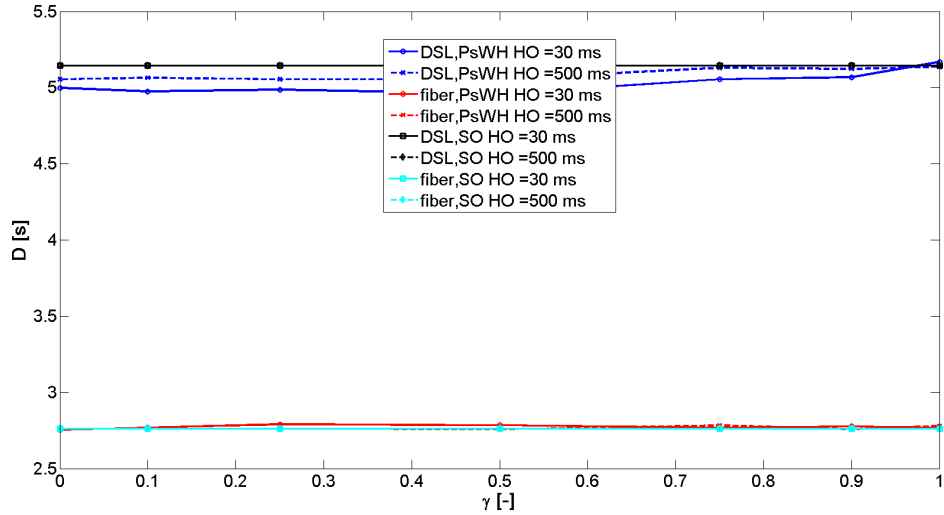


Figure 6.12: Gain in delay against SO for request size of 300 kB.

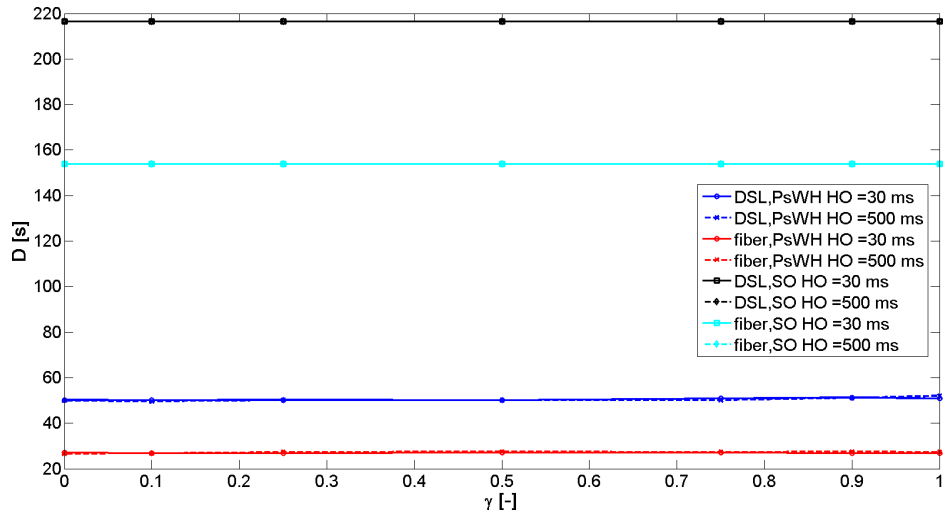


Figure 6.13: Gain in delay against SO for request size of 3 MB.

Energy requirements are compared in Figures 6.14 for load of 300 kB and 6.15 for load of 3 MB. For the 300 kB, PSwH brings no improvement for fiber backhaul, but improvement of 400 % is seen for DSL backhaul. As the  $\gamma \rightarrow 1$  in case of DSL with handover duration of 500 ms, the PSwH provides same results as the SO, because handover duration is high in comparison of data transmission and thus the PSwH uses the same paths as does the SO. In case of load of 3 MB, the PSwH provides lower energy consumption by up to 300 %.

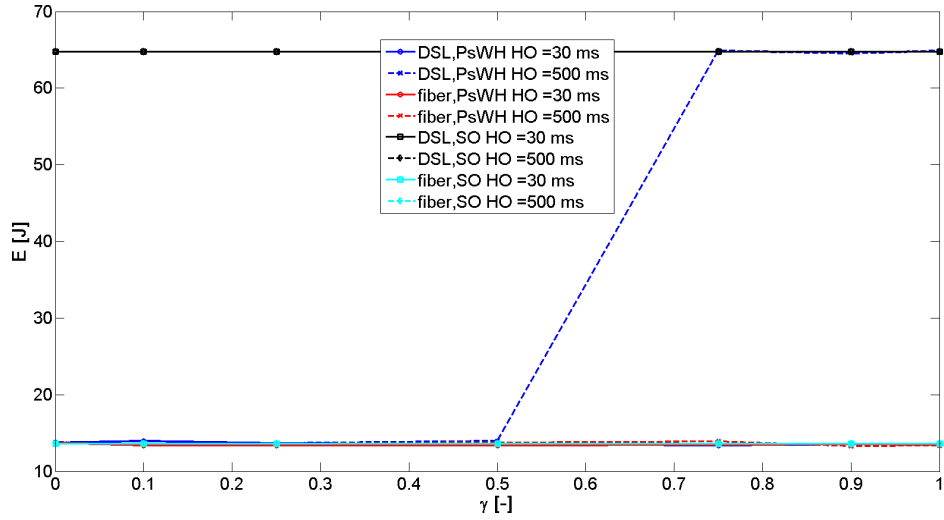


Figure 6.14: Gain in energy against SO for request size of 300 kB.

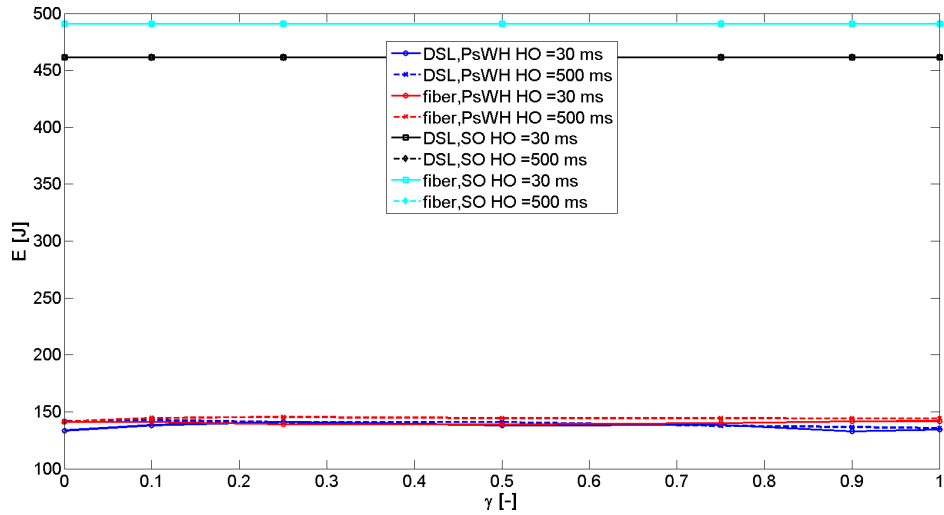


Figure 6.15: Gain in energy against SO for request size of 3 MB.

In comparison of the UE satisfaction for load of 300 kB no improvement is seen as shown in Figure 6.16, however in case of requested load 3 MB, the PSwH provides up to 40 % increase in satisfaction as shown in Figure 6.17. If  $T_{req} = 150s$  is selected, each UE using the PSwH is satisfied while in case of SO, 30 % and 40 % of UEs are still not satisfied for fiber and DSL backhaul respectively.

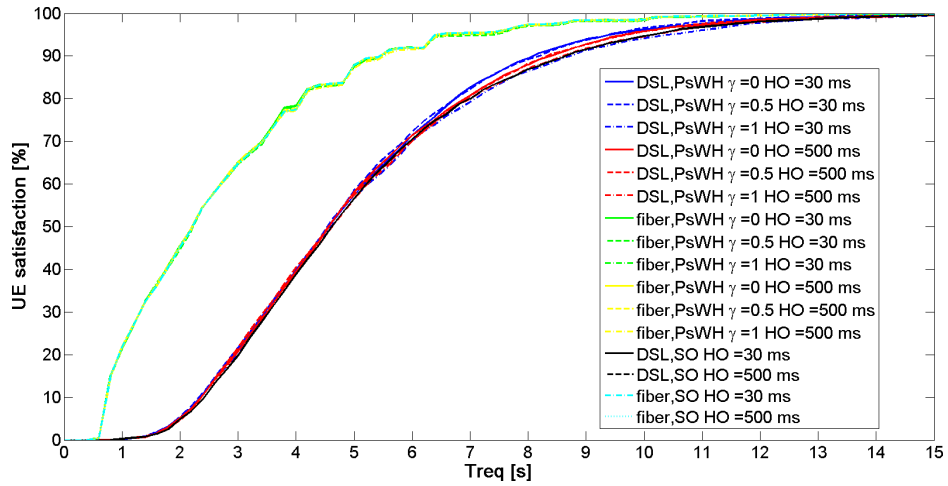


Figure 6.16: UE satisfaction for request size of 300 kB.

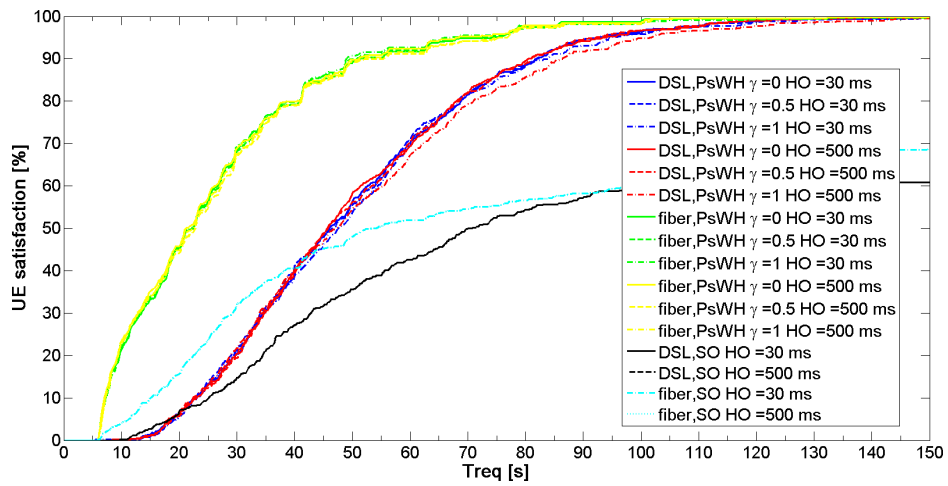


Figure 6.17: UE satisfaction for request size of 3 MB.

In Figures 6.18 and 6.19 is seen decrease of additional handover by the PSwH as the  $\gamma \rightarrow 1$ , as the handover consumption becomes unwanted to lower energy consumption when energy efficiency is required.



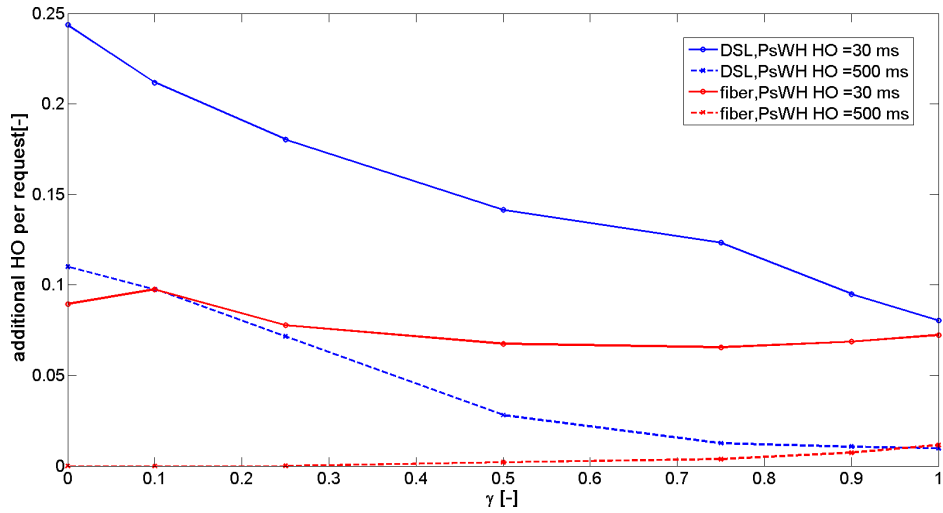


Figure 6.18: Number of additional handovers for request size of 300 kB.

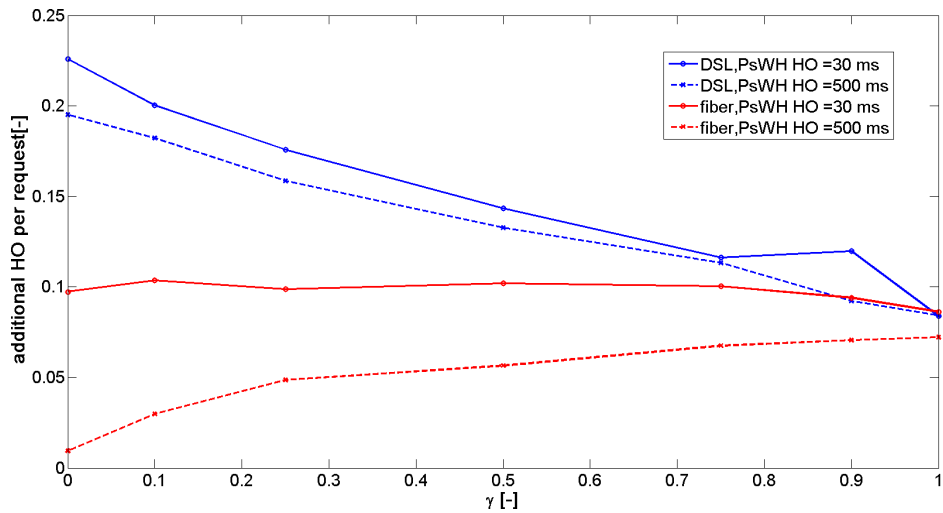


Figure 6.19: Number of additional handovers for request size of 3 MB.

## 6.2.2 Shared radio resources

In this section resources on the radio are shared in the same manner as on a backhaul.

For load of 300 kB, only 5 % improvement of D using the PSwH for DSL backhaul is seen as shown in Figure 6.20. In case of load of 3 MB, the PSwH provides D over 400 % smaller than the SO does in case of DSL backhaul and almost up to 400 % for the fiber backhaul as shown in Figure 6.21.

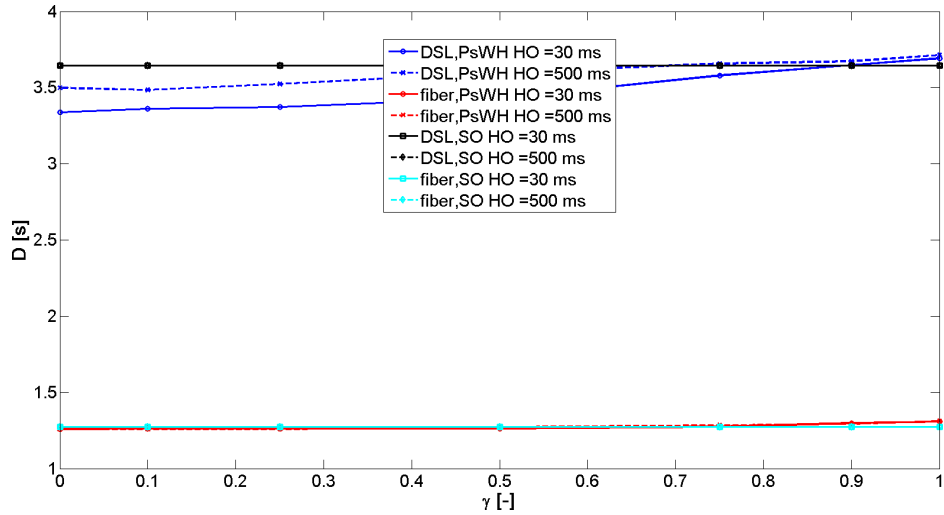


Figure 6.20: Gain in energy against SO for request size of 300 kB.

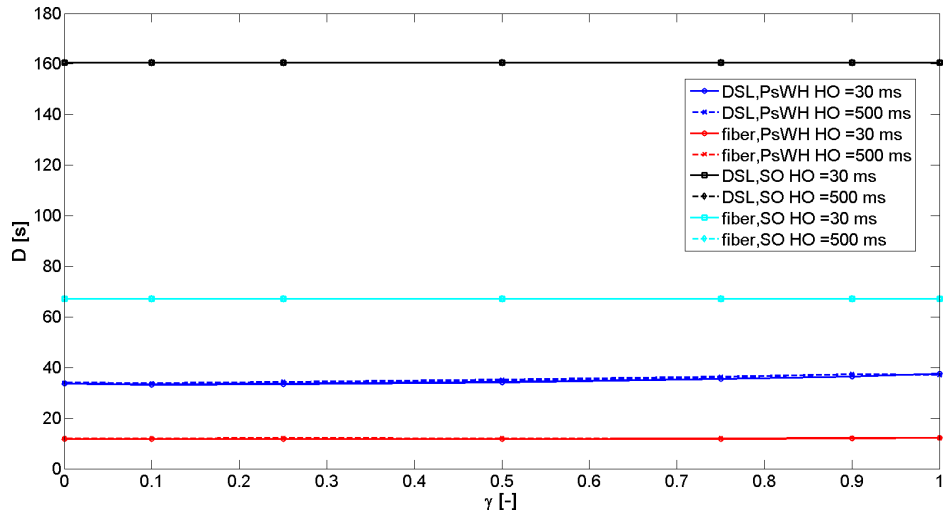


Figure 6.21: Gain in energy against SO for request size of 3 MB.

In E comparison, we see in Figure 6.22 how requests create different network flow and make  $\gamma = 1$  not the best energy efficient ratio. If DSL backhaul is used, the PSwH provides better results in units of percents. In case of fiber backhaul, the PSwH requires about 2 % more E than SO does.

When load of 3 MB is required, Figure 6.23, the PSwH consumes over 500 % less energy than SO does.

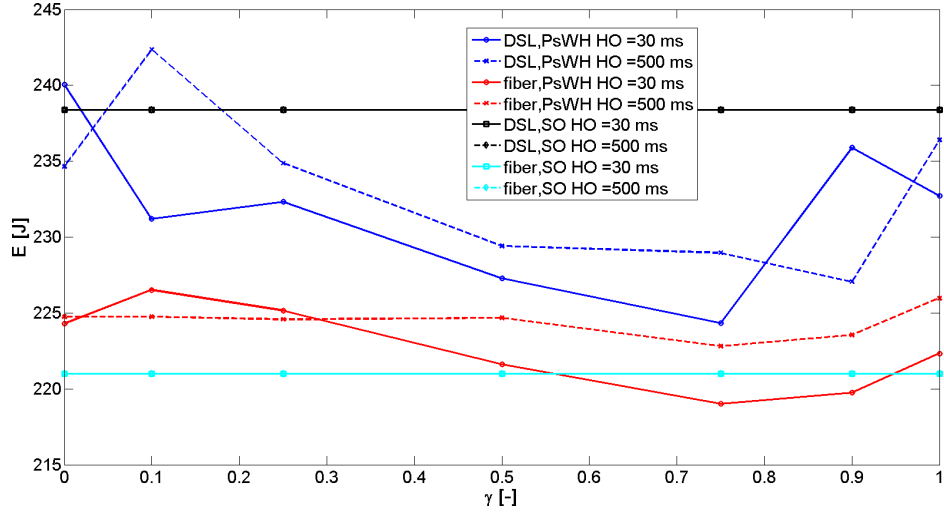


Figure 6.22: Gain in delay against SO for request size of 300 kB.

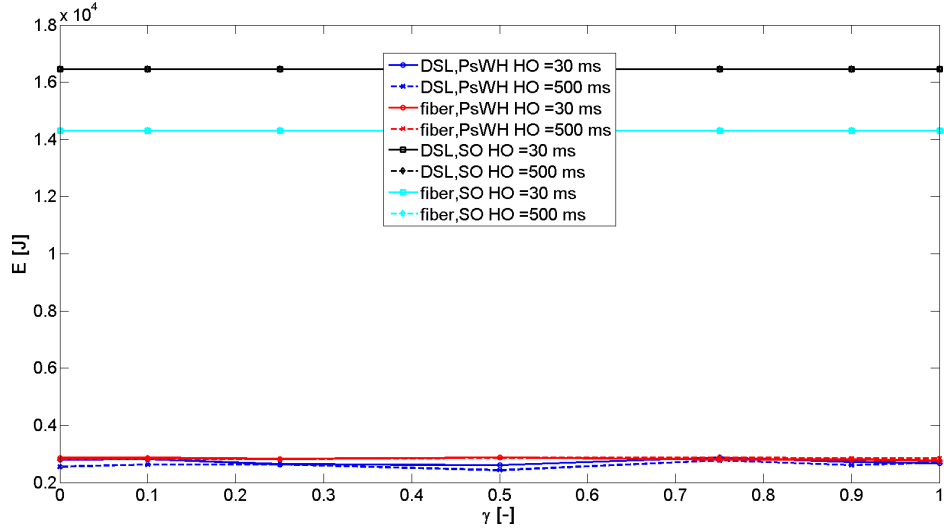


Figure 6.23: Gain in delay against SO for request size of 3 MB.

In UE satisfaction comparison for load of 300 kB, in Figure 6.23, no difference between the PSwH and the SO can be seen for the fiber backhaul, while for the DSL backhaul, up to 10 % increase in UE satisfaction is seen for the  $T_{req} = 5s$ .

When load of 3 MB is required, in Figure 6.25 for  $T_{req} = 100s$  about 99.5 % UEs are satisfied if using the PSwH while almost 30 % requests are still not satisfied using the SO for fiber backhaul. For DSL backhaul, we see improvement by almost 45 % if UE uses the PSwH instead of the SO.

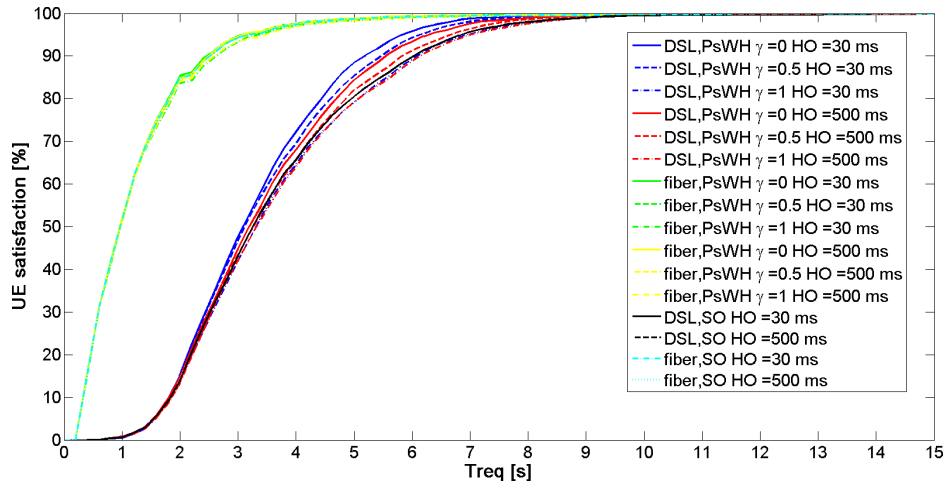


Figure 6.24: UE satisfaction for request size of 300 kB.

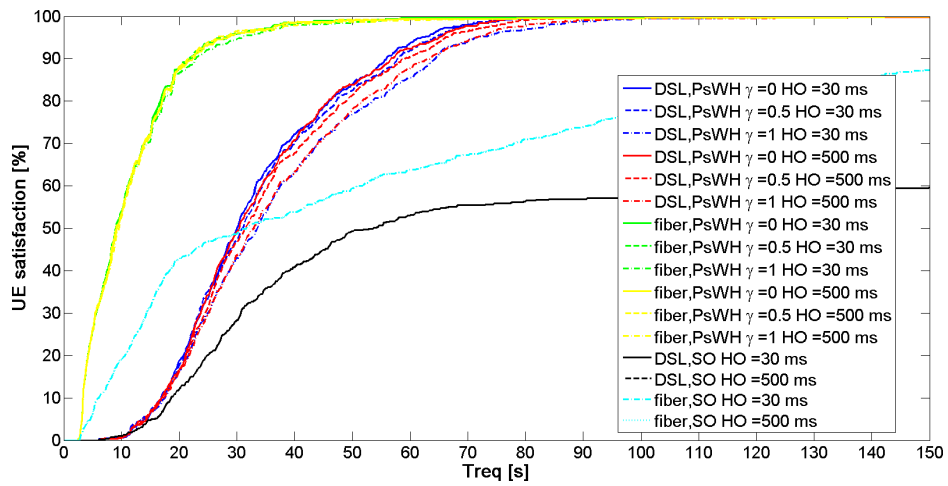


Figure 6.25: UE satisfaction for request size of 3 MB.

Number of additional handover decreases as shown in Figures 6.26 and 6.27. As  $\gamma \rightarrow 1$ , for DSL backhaul for both loads, decrease is seen. For fiber backhaul, we see small increase as the UE uses different path with lower energy consumption.

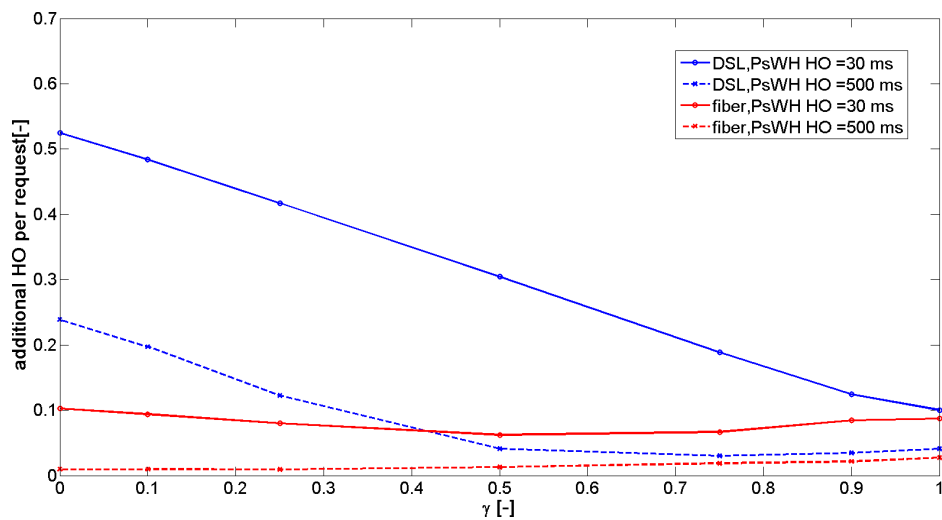


Figure 6.26: Number of additional handovers for request size of 300 kB.

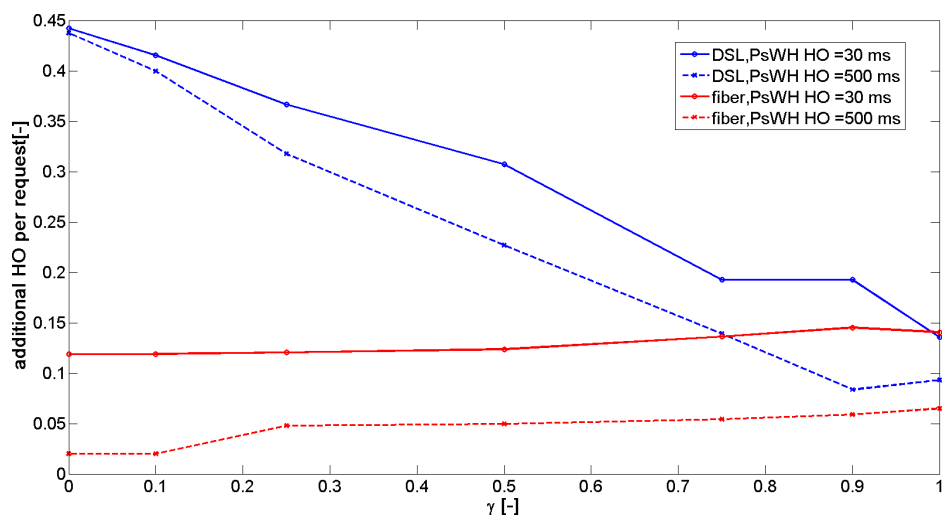


Figure 6.27: Number of additional handovers for request size of 3 MB.

# Conclusion

In this thesis, femto-cloud was described and new algorithm for selection of path from the UE to cloud-enhanced small cells is proposed named Path Selection with Handover (PSwH). The proposed algorithm force handover to the computing cell if it is efficient by means of the overall transmission delay (considering radio and backhaul) or energy.

From the UE point of view, the proposed algorithm is efficient especially for capacity limited backhauls (e.g., DSL). In this case, it reduces transmission delay by up to 9% if UE's energy consumption is of lower preference and increase in energy spent for transmission by 5.5% is not critical. If energy consumption is constraint, the proposed algorithm still reduces transmission delay by 6.7% while energy required for transmission is at the same level as for the conventional approach. For backhaul of high capacity (such as optical fiber), the delay can be reduced up to 4.7% while energy consumption is not raised. In addition, the user satisfaction with delay requirements is increased by up to 6.5% and 1.8% for DSL and optical fiber backhauls, respectively. From the point of view of UE, algorithm provide improvement especially for the DSL and similar backhauls.

From the network point of view, for the load of 300 kB improvements of few percents can be seen, however for the load of 3 MB, decrease of delay up to 400 % and 500 % is seen for the both backhaul connections if required load is 3 MB. As for the energy consumption, improvements in units of percents is seen for the load of 300 kB, while for the load of 3 MB, improvement (decrease in consumed energy) rises up to 500 %. From the point of UE satisfaction, for the load of 300 kB, improvement is in percents while for the load of 3MB, improvement is up to 40 %. From above results we can conclude that proposed algorithm provides noticeable improvement over the existing one in each aspect, especially if load of requests becomes larger in case of network point of view.

In the future, we will focus on extension of the proposed algorithm to CoMP communication and to combination with possible migrating of VMs among SCeNBs in order to shorten delay. Also focus on higher user mobility to predict and select paths with knowledge on the user movement will be made.

# Bibliography

- [1] 3GPP, “3gpp ts 36.213, technical specification group radio access network; evolved universal terrestrial radio access (e-utra) and evolved universal terrestrial radio access network (e-utran);overall description; stage 2 (release 12),” tech. rep., 3rd Generation Partnership Project (3GPP), 2014.
- [2] S. Ahmadi, *LTE-Advanced: A Practical Systems Approach to Understanding 3GPP LTE Releases 10 and 11 Radio Access Technologies*. Elsevier Science, 2013.
- [3] 3GPP, “3gpp ts 36.101, technical specification group radio access network; evolved universal terrestrial radio access (e-utra); user equipment (ue) radio transmission and reception (release 12),” tech. rep., 3rd Generation Partnership Project (3GPP), 2014.
- [4] S. Carlaw, “Connected world of tomorrow, predictions for 2014 and 2015,” tech. rep., ABI research, 2014.
- [5] M. Barbera, S. Kosta, A. Mei, and J. STEFA, “To offload or not to offload? the bandwidth and energy costs of mobile cloud computing,” in *INFOCOM, 2013 Proceedings IEEE*, pp. 1285–1293, April 2013.
- [6] S. C. Forum, “Small cell market highlights,” *Small Cell Forum*, 2014.
- [7] M. P. P. M. F. L. P. F. G. M. G. J. V. A. W. E. C. F. Lobillo, Z. Becvar, “An architecture for mobile computation offloading on cloud-enabled lte small cells,” in *IEEE WCNC2014 Workshops*, pp. 1285–1293, April 2014.
- [8] S. Barbarossa, S. Sardellitti, and P. Di Lorenzo, “Computation offloading for mobile cloud computing based on wide cross-layer optimization,” in *Future Network and Mobile Summit (FutureNetworkSummit), 2013*, pp. 1–10, July 2013.
- [9] b. t. y. m. V. Di Valerio, F. Lo Presti
- [10] J. Al-Karaki and A. Kamal, “Routing techniques in wireless sensor networks: a survey,” *Wireless Communications, IEEE*, vol. 11, pp. 6–28, Dec 2004.
- [11] M. Marina and S. Das, “On-demand multipath distance vector routing in ad hoc networks,” in *Network Protocols, 2001. Ninth International Conference on*, pp. 14–23, Nov 2001.
- [12] M. Medley, “Robust on-demand multipath routing with dynamic path upgrade for delay-sensitive data over ad hoc networks,” *Journal of Computer Networks and Communications*, vol. 2013, 2013.

- 
- [13] H. Holma and A. Toskala, *LTE for UMTS OFDMA and SC-FDMA Based Radio Access*. John Wiley & sons Ltd., 2009.
- [14] 3GPP, “3gpp ts 36.213, technical specification group radio access network; evolved universal terrestrial radio access (e-utra); physical layer procedures (release 11),” tech. rep., 3rd Generation Partnership Project (3GPP), 2013.
- [15] 3GPP, “3gpp ts 23.002, technical specification group services and system aspects; network architecture (release 12),” tech. rep., 3rd Generation Partnership Project (3GPP), 2014.
- [16] 3GPP, “3gpp ts 23.401, technical specification group services and system aspects; general packet radio service (gprs) enhancements for evolved universal terrestrial radio access network (e-utran) access (release 12),” tech. rep., 3rd Generation Partnership Project (3GPP), 2013.
- [17] 3GPP, “3gpp ts 36.331, technical specification group radio access network; evolved universal terrestrial radio access (e-utra); radio resource control (rrc); protocol specification (release 11),” tech. rep., 3rd Generation Partnership Project (3GPP), 2013.
- [18] CISCO, “Cisco visual networking index: Global mobile data traffic forecast update, 2013–2018,” 2014.
- [19] J. Zhang and G. de la Roche, *Femtocells: Technologies and deployment*. John Wiley & sons Ltd., 2010.
- [20] S. C. Forum, “Small cells – big ideas, how small cells left home – and where they’re going next,” *Small Cell Forum*, 2014.
- [21] S. C. Forum, “Small cells – urban small cell network architectures,” *Small Cell Forum*, 2014.
- [22] S. C. Forum, “Small cells – synchronisation for lte small cells,” *Small Cell Forum*, 2013.
- [23] 3GPP, “3gpp tr 36.922, technical specification group radio access network; evolved universal terrestrial radio access (e-utra); tdd home enode b (henb) radio frequency (rf) requirements analysis (release 11),” tech. rep., 3rd Generation Partnership Project (3GPP), 2012.
- [24] F. L. Vilela, “D22: Design of network architecture for femto-cloud computing,” tech. rep., Project TROPIC deliverable, 2013.
- [25] O. Munoz, A. Pascual-Iserte, and J. Vidal, “Joint allocation of radio and computational resources in wireless application offloading,” in *Future Network and Mobile Summit (FutureNetworkSummit)*, 2013, pp. 1–10, July 2013.
- [26] G. Bolch, S. Greiner, H. de Meer, and K. S. Trivedi, *Queueing Networks and Markov Chains: Modeling and Performance Evaluation with Computer Science Applications*. New York, NY, USA: Wiley-Interscience, 1998.



- 
- [27] 3GPP, “3gpp ts 36.314, technical specification group radio access network; evolved universal terrestrial radio access (e-utra); layer 2 - measurements (release 11),” tech. rep., 3rd Generation Partnership Project (3GPP), 2012.
- [28] 3GPP, “3gpp tr-36.814, technical specification group radio access network; evolved universal terrestrial radio access (e-utra); further advancements for e-utra physical layer aspects (release 9),” tech. rep., 3rd Generation Partnership Project (3GPP), 2010.
- [29] 3GPP, “3gpp ts 29.212, technical specification group radio access network; universal mobile telecommunications system (umts);lte;policy and charging control over gx reference point (release 8),” tech. rep., 3rd Generation Partnership Project (3GPP), 2009.
- [30] A. Agustin, “Scenario, requirements and first business model analysis,” tech. rep., Deliverable D21 of ICT-248891 STP FREEDOM project, 2010.
- [31] I. Forkel, M. Schinnenburg, and M. Ang, “Generation of Two-Dimensional Correlated Shadowing for Mobile Radio Network Simulation,” in *Proceedings of The 7th International Symposium on Wireless Personal Multimedia Communications, WPMC 2004*, (Abano Terme (Padova), Italy), Sept. 2004.
- [32] C. Mehlhruher, J. Colom Ikuno, M. Simko, S. Schwarz, M. Wrulich, and M. Rupp, “The vienna lte simulators - enabling reproducibility in wireless communications research,” *EURASIP Journal on Advances in Signal Processing*, vol. 2011, no. 1, p. 29, 2011.
- [33] D. N. Meghanathan, “Mobility models for wireless ad hoc networks,” Presented at the REU 2010, Jackson State University, 2010.
- [34] H. Claussen, L. T. W. Ho, and L. Samuel, “Self-optimization of coverage for femto-cell deployments,” in *Wireless Telecommunications Symposium, 2008. WTS 2008*, pp. 278–285, April 2008.
- [35] M. Lauridsen, A. Jensen, and P. Mogensen, “Reducing lte uplink transmission energy by allocating resources,” in *Vehicular Technology Conference (VTC Fall), 2011 IEEE*, pp. 1–5, Sept 2011.
- [36] M. Lauridsen, “An empirical lte smartphone power model with a view to energy efficiency evolution,” *Intel Technology Journal*, 2014.
- [37] E. Tejaswi and S. B, “Survey of power control schemes for lte uplink,” 2013.
- [38] 3GPP, “3gpp ts 23.009, technical specification group core network and terminals; handover procedures (release 11),” tech. rep., 3rd Generation Partnership Project (3GPP), 2012.

# Appendices

Table 8.1: E-UTRA frequency bands [3]

E-UTRA Operating Band	Uplink (UL) operating band BS receive UE transmit	Downlink (DL) operating band BS transmit UE receive	Duplex Mode
	$f_{low} - f_{high}$	$f_{low} - f_{high}$	
1	1920 MHz – 1980 MHz	2110 MHz – 2170 MHz	FDD
2	1850 MHz – 1910 MHz	1930 MHz – 1990 MHz	FDD
3	1710 MHz – 1785 MHz	1805 MHz – 1880 MHz	FDD
4	1710 MHz – 1755 MHz	2110 MHz – 2155 MHz	FDD
5	824 MHz – 849 MHz	869 MHz – 894 MHz	FDD
6	830 MHz – 840 MHz	875 MHz – 885 MHz	FDD
7	2500 MHz – 2570 MHz	2620 MHz – 2690 MHz	FDD
8	880 MHz – 915 MHz	925 MHz – 960 MHz	FDD
9	1749.9 MHz – 1784.9 MHz	1844.9 MHz – 1879.9 MHz	FDD
10	1710 MHz – 1770 MHz	2110 MHz – 2170 MHz	FDD
11	1427.9 MHz – 1447.9 MHz	1475.9 MHz – 1495.9 MHz	FDD
12	699 MHz – 716 MHz	729 MHz – 746 MHz	FDD
13	777 MHz – 787 MHz	746 MHz – 756 MHz	FDD
14	788 MHz – 798 MHz	758 MHz – 768 MHz	FDD
15	Reserved	Reserved	FDD
16	Reserved	Reserved	FDD
17	704 MHz – 716 MHz	734 MHz – 746 MHz	FDD
18	815 MHz – 830 MHz	860 MHz – 875 MHz	FDD
19	830 MHz – 845 MHz	875 MHz – 890 MHz	FDD
20	832 MHz – 862 MHz	791 MHz – 821 MHz	FDD
21	1447.9 MHz – 1462.9 MHz	1495.9 MHz – 1510.9 MHz	FDD
22	3410 MHz – 3490 MHz	3510 MHz – 3590 MHz	FDD
23	2000 MHz – 2020 MHz	2180 MHz – 2200 MHz	FDD
24	1626.5 MHz – 1660.5 MHz	1525 MHz – 1559 MHz	FDD
25	1850 MHz – 1915 MHz	1930 MHz – 1995 MHz	FDD
33	1900 MHz – 1920 MHz	1900 MHz – 1920 MHz	TDD
34	2010 MHz – 2025 MHz	2010 MHz – 2025 MHz	TDD
35	1850 MHz – 1910 MHz	1850 MHz – 1910 MHz	TDD
36	1930 MHz – 1990 MHz	1930 MHz – 1990 MHz	TDD
37	1910 MHz – 1930 MHz	1910 MHz – 1930 MHz	TDD
38	2570 MHz – 2620 MHz	2570 MHz – 2620 MHz	TDD
39	1880 MHz – 1920 MHz	1880 MHz – 1920 MHz	TDD
40	2300 MHz – 2400 MHz	2300 MHz – 2400 MHz	TDD
41	2496 MHz – 2690 MHz	2496 MHz – 2690 MHz	TDD
42	3400 MHz – 3600 MHz	3400 MHz – 3600 MHz	TDD
43	3600 MHz – 3800 MHz	3600 MHz – 3800 MHz	TDD

Table 8.2: Assigned SINR to CQI

CQI index	SNR [dB]	Modulation	Coding rate x 1024	Bits per resource element (modulation efficiency)
1	-6.9	QPSK	78	0.1523
2	-5.15	QPSK	120	0.2344
3	-3.2	QPSK	193	0.377
4	-1.3	QPSK	308	0.6016
5	0.8	QPSK	449	0.877
6	2.7	QPSK	602	1.1758
7	4.7	16QAM	378	1.4766
8	6.5	16QAM	490	1.9141
9	8.6	16QAM	616	2.4063
10	10.37	64QAM	466	2.7305
11	12.29	64QAM	567	3.3223
12	14.17	64QAM	666	3.9023
13	15.89	64QAM	772	4.5234
14	17.81	64QAM	873	5.1152
15	19.83	64QAM	948	5.5547